



Priyanka Priyanka · Fateh Mebarek-Oudina · Saroj Sahani ·
Shelly Arora

Travelling wave solution of fourth order reaction diffusion equation using hybrid quintic hermite splines collocation technique

Received: 17 May 2023 / Accepted: 21 March 2024
© The Author(s) 2024

Abstract Fourth order extended Fisher Kolmogorov reaction diffusion equation has been solved numerically using a hybrid technique. The temporal direction has been discretized using Crank Nicolson technique. The space direction has been split into second order equation using twice continuously differentiable function. The space splitting results into a system of equations with linear heat equation and non linear reaction diffusion equation. Quintic Hermite interpolating polynomials have been implemented to discretize the space direction which gives a system of collocation equations to be solved numerically. The hybrid technique ensures the fourth order convergence in space and second order in time direction. Unconditional stability has been obtained by plotting the eigen values of the matrix of iterations. Travelling wave behaviour of dependent variable has been obtained and the computed numerical values are shown by surfaces and curves for analyzing the behaviour of the numerical solution in both space and time directions.

Mathematics Subject Classification 35B25 · 35C07 · 65D07 · 65M06 · 65N35

1 Introduction

Different forms of non-linear PDEs like advection–diffusion, reaction–diffusion or many more have been modelled and analyzed corresponding to some real-life phenomenon or scientific processes so far [2, 4, 16, 24, 34, 44]. Non-linear reaction diffusion equations having fourth order derivative terms, frame problems in the vast category of fields under science and engineering. These equations occur in both the form of ordinary differential equation (ODE) and partial differential equation (PDE). The wide applications of these problems have made it the topic of research worldwide since long ago. In [62] a non-linear PDE modelling the under-ground water flow problem, which is a serious problem for the living-beings has been considered. In [59] a non-linear

Priyanka Priyanka, Fateh Mebarek-Oudina and Saroj Sahani contributed equally to this work.

P. Priyanka · S. Arora (✉)
Department of Mathematics, Punjabi University, Patiala, Punjab 147002, India
E-mail: aroshelly@pbi.ac.in

P. Priyanka
E-mail: priyanka_rs@pbi.ac.in

F. Mebarek-Oudina
Department of Physics, University of 20 Août 1955-Skikda, Road El-Hadaek, B.P. 26, 21000 Skikda, Algeria
E-mail: f.mebarek_oudina@univ-skikda.dz

S. Sahani
Department of Mathematics, South Asian University, Rajpur Road, Maidan Garhi, New Delhi, Delhi 110068, India
E-mail: sarojkumar@sau.ac.in



PDE modelling the propagation of optic pulses in optic fibers has been solved analytically. Applications of various non-linear partial differential equations and non availability of the compact form of solution in most of the cases, demands an efficient technique for analysing the phenomenon. Earlier, non-linear PDEs have been treated numerically as well as analytically [1, 38] to study the solution behaviour of these problems. Various forms of non-linear reaction–diffusion equations having vast field of applications has been studied so far [14, 35, 42, 66]. Extended Fisher Kolmogorov (EFK) equation is an example of such type of reaction diffusion equation involving linear diffusion term and non-linear logistic term $f(u)$. Consider the general form of non-linear reaction diffusion fourth order parabolic partial differential equation.

$$u_t + \varepsilon u_{\zeta\zeta\zeta\zeta} - u_{\zeta\zeta} + f(u) = 0 \quad (\zeta, t) \in (a, b) \times (0, T], \quad (1)$$

with $\varepsilon > 0$ and $f(u)$ as a non-linear polynomial function of u .
Initially, $u(\zeta, 0) = u_0(\zeta)$ $\zeta \in (a, b)$.

The boundary conditions are defined as:

$$\begin{aligned} u(a, t) &= g_1(t) & u(b, t) &= g_2(t) \\ u_{\zeta\zeta}(a, t) &= g_3(t) & u_{\zeta\zeta}(b, t) &= g_4(t). \end{aligned} \quad (2)$$

where, $g_1(t)$, $g_2(t)$, $g_3(t)$ and $g_4(t)$ are continuous functions of t and $f(u) = u - u^m$, $m > 1$. For $f(u) = u - u^3$, the Eq. (1) is introduced as Extended Fisher–Kolmogorov (EFK) equation with perturbation parameter $0 \leq \varepsilon \leq 1$. For $\varepsilon = 0$, Eq. (1) is standard Fisher–Kolmogorov equation given by Fisher and Kolmogorov which models complex biological processes in gene theory [6, 28]. The requirement $\varepsilon > 0$ is chosen for stability of Eq. (1) at short wavelength [23]. Various physical phenomenon like pattern formation due to propagating fronts [23, 64], spatial temporal chaos in bi-stable systems [19], chemical waves [27], transition of phase and propagation of fronts near a Lipschitz point [33, 67], instabilities in liquid crystals [18, 67], propagating waves in reaction–diffusion systems [29, 55] have been framed by Eq. (1) which approaches the amplitude near certain degenerate points [57]. Also, in [56], the transition from periodic patterns by Ginzburg–Landau equation to the multi-bump solutions predicted by EFK equation has been discussed. Periodicity, chaotic, stationary behavior, uniqueness of the solution and existence of kinks, travelling wave solutions etc. have also been considered [22, 47, 49–51, 57, 63].

In literature, non-linear parabolic PDEs have been analyzed by different numerical techniques [9, 53]. Various elliptic non-linear second order PDEs having compact form of solution have been treated with generalized finite difference method given in [30]. Due to the complex nature, compact form of solution exists only for some non-linear higher order PDEs. Complexity of the equation enhances the requirement of numerical techniques. EFK equation has been analyzed by variational method for investigating the nature of saddle-focus equilibria connections [36]. Topological shooting method has been applied for the existence of kinks and analyzing their properties [48]. Numerically, it has been implemented with the differential quadrature method [13, 54], orthogonal cubic spline collocation method [21], quintic B-spline collocation method [46], mixed finite element method [65], quintic trigonometric differential quadrature method [7], finite element method [20], Galerkin approximation technique [31], compact difference method [37] etc. Quasi-Exact solution has been obtained in [39]. Local radial basis function, finite difference method [25] has also been implemented for numerical solution of EFK equation.

In present study collocation method with Hermite splines has been discussed. Collocation technique is basically a three-step process

1. Suitable choice of the finite degree polynomial lying in finite dimensional space for the discretization process.
2. Suitable choice of collocation points for space discretization.
3. Making that polynomial solution to satisfy the equation at the collocation points.

In the present study, a hybrid Crank–Nicolson quintic Hermite spline method accomplished by the reduction of the order of the aforementioned differential equation has been considered. The considered mesh is uniform in both space and time directions. This technique improves the efficiency of collocation technique in approximation by interpolating the function and its derivatives up-to second order at nodal points. Quintic Hermite splines are simple, smooth, easy to implement and can be implemented to the variety of boundary value problems having high order and high degree of non-linearity. Travelling wave behaviour has been analysed with different values of various parameters and the non-linear function $f(u)$. Quintic Hermite splines (QHS) provide super convergence up to fourth order in spatial direction and Crank–Nicolson scheme is second order

convergent. Earlier, the technique has been applied to second order, singularly perturbed non-linear partial differential equations [8, 11, 12]. The computational work for the approximation of fully discrete system is comparatively easy to program.

The paper is fabricated by the introduction of EFK equation in Sect. 1. Second order splitting method has been explained briefly under Sect. 2. Hybrid quintic Hermite spline collocation method has been elaborated in Sect. 3 whereas in Sect. 4 stability analysis has been discussed. The existence of error bounds and convergence analysis has been discussed in Sect. 5. The application of QHS with Crank Nicolson scheme has been discussed in Sect. 6 and the conclusions of the entire study is given in Sect. 7.

2 Second order splitting of EFK equation

Fourth order non-linear equations involve concerned differential equation and four constraints. To apply any numerical technique, these constraints play an important role to discretize the equation. Quintic Hermite splines by construction involve the discretized form of the differential equation at collocation points and two constraints at the boundary of the interpolating polynomial. Therefore, to apply quintic Hermite splines on fourth order differential equation, it must be split into second order differential equation by introducing second order continuously differentiable function to reduce the number of constraints to two for each interpolating polynomial.

Theorem 2.1 [5] *Any Hermite interpolation problem of any order $n \in N$ is applicable on two point boundary value problems.*

Consider the non-linear EFK type Eq. (1). For the implementation of proposed technique, a twice continuously differentiable function $v(\zeta, t)$ has been introduced such that:

$$v(\zeta, t) = -u_{\zeta\zeta}(\zeta, t).$$

On substitution [26], the induced coupled system of differential equations is obtained as under:

$$v + u_{\zeta\zeta} = 0, \tag{3}$$

$$u_t - \varepsilon v_{\zeta\zeta} + v + f(u) = 0, \tag{4}$$

with $f(u) = u - u^m$, subject to the following initial and boundary conditions:

$$u(\zeta, 0) = u_0(\zeta), \tag{5}$$

$$u(a, t) = g_1(t) \quad u(b, t) = g_2(t), \tag{6}$$

$$v(a, t) = 0 \quad v(b, t) = 0. \tag{7}$$

Hence, a fourth order equation has been reduced to a system of equations with one equation is linear and another is semi-linear. This splitting of non-linear EFK equation gives a semi-linear parabolic equation in two function u and v .

3 Hybrid quintic hermite spline collocation method

The hybrid technique consists of discretization using time and space semi-discretizing techniques. This two-step process has been implemented to the second order coupled system of singularly perturbed PDEs:

3.1 Time discretization

For discretization in time direction, the Crank–Nicolson scheme has been followed as a special case of weighted finite difference scheme [60]. This Crank–Nicolson scheme is based on the concept of nearest neighbourhood points to analyse the behaviour without any jump in time direction [15]. For implementation of the technique to the reduced coupled system for EFK equation, let v^{n+1} and u^{n+1} be the approximating polynomial function

at time step t_{n+1} . Also, let $\Delta t = T/M$, $M > 0$ then $t_n = n\Delta t$ for $n = 0, 1, 2, \dots, M$. The semi-discretized form of the coupled system follows as:

$$v^{n+\frac{1}{2}} = -u_{\zeta\zeta}^{n+\frac{1}{2}}, \tag{8}$$

$$\frac{u^{n+1} - u^n}{\Delta t} = \varepsilon v_{\zeta\zeta}^{n+\frac{1}{2}} - v^{n+\frac{1}{2}} - (u^n - u)^{n+\frac{1}{2}}, \tag{9}$$

with corresponding boundary conditions are given by Eqs. (6) and (7), respectively. For any function F ,

$$F^{n+\frac{1}{2}} = \frac{F^{n+1} + F^n}{2}. \tag{10}$$

3.2 Space discretization

Let $\Pi : a = \zeta_0 < \zeta_1 < \zeta_2 < \dots < \zeta_n = b$, $\zeta_i' s \in I$ be the partition of the domain $I = [a, b]$ and let $h_i = \zeta_{i+1} - \zeta_i$ and I_i denotes $[\zeta_i, \zeta_{i+1}]$. Corresponding to each subinterval I_i , six collocation points have been taken including two boundary or node points. Collocation points are the roots of shifted Legendre polynomial of order six which are not equidistant to the average and the details of these collocation points is given elsewhere [10].

In space direction, the quintic Hermite interpolating polynomials $P_i(\eta)$, $\bar{P}_i(\eta)$ and $\bar{\bar{P}}_i(\eta)$ are introduced to approximate the trial function within each partition I_i of the domain. The approximate function is considered as:

$$u(\zeta) = u(\zeta_i) \sum_{i=1}^2 P_i(\zeta) + u'(\zeta_i) \sum_{i=1}^2 \bar{P}_i(\zeta) + u''(\zeta_i) \sum_{i=1}^2 \bar{\bar{P}}_i(\zeta), \tag{11}$$

where $P_i(\zeta)$ interpolates the function $u(\zeta)$ at the nodal points of the sub-interval I_i and $\bar{P}_i(\zeta)$, $\bar{\bar{P}}_i(\zeta)$ interpolates slope and curvature at the nodal points, respectively.

$$\begin{aligned}
 Q_i(\zeta) &= \begin{cases} 6 \frac{(\zeta_{i+1}-\zeta)^5}{(\zeta_{i+1}-\zeta_i)^5} - 15 \frac{(\zeta_{i+1}-\zeta)^4}{(\zeta_{i+1}-\zeta_i)^4} + 10 \frac{(\zeta_{i+1}-\zeta)^3}{(\zeta_{i+1}-\zeta_i)^3} & \zeta_i \leq \zeta \leq \zeta_{i+1} \\ 6 \frac{(\zeta-\zeta_{i-1})^5}{(\zeta_i-\zeta_{i-1})^5} - 15 \frac{(\zeta-\zeta_{i-1})^4}{(\zeta_i-\zeta_{i-1})^4} + 10 \frac{(\zeta-\zeta_{i-1})^3}{(\zeta_i-\zeta_{i-1})^3} & \zeta_{i-1} \leq \zeta \leq \zeta_i \\ 0 & \text{otherwise} \end{cases} \\
 \bar{Q}_i(\zeta) &= \begin{cases} 3 \frac{(\zeta_{i+1}-\zeta)^5}{(\zeta_{i+1}-\zeta_i)^4} - 7 \frac{(\zeta_{i+1}-\zeta)^4}{(\zeta_{i+1}-\zeta_i)^3} + 4 \frac{(\zeta_{i+1}-\zeta)^3}{(\zeta_{i+1}-\zeta_i)^2} & \zeta_i \leq \zeta \leq \zeta_{i+1} \\ -3 \frac{(\zeta-\zeta_{i-1})^5}{(\zeta_i-\zeta_{i-1})^4} + 7 \frac{(\zeta-\zeta_{i-1})^4}{(\zeta_i-\zeta_{i-1})^3} - 4 \frac{(\zeta-\zeta_{i-1})^3}{(\zeta_i-\zeta_{i-1})^2} & \zeta_{i-1} \leq \zeta \leq \zeta_i \\ 0 & \text{otherwise} \end{cases} \\
 \bar{\bar{Q}}_i(\zeta) &= \begin{cases} \frac{(\zeta_{i+1}-\zeta)^5}{2(\zeta_{i+1}-\zeta_i)^3} - \frac{(\zeta_{i+1}-\zeta)^4}{(\zeta_{i+1}-\zeta_i)^2} + \frac{(\zeta_{i+1}-\zeta)^3}{2(\zeta_{i+1}-\zeta_i)} & \zeta_i \leq \zeta \leq \zeta_{i+1} \\ \frac{(\zeta-\zeta_{i-1})^5}{2(\zeta_i-\zeta_{i-1})^3} - \frac{(\zeta-\zeta_{i-1})^4}{(\zeta_i-\zeta_{i-1})^2} + \frac{(\zeta-\zeta_{i-1})^3}{2(\zeta_i-\zeta_{i-1})} & \zeta_{i-1} \leq \zeta \leq \zeta_i \\ 0 & \text{otherwise.} \end{cases} \tag{12}
 \end{aligned}$$

To apply orthogonal collocation, within each subinterval I_i a new variable ω is introduced such that $\omega = \frac{(\zeta-\zeta_i)}{h_i}$, where ω varies from 0 to 1 as ζ varies from ζ_i to ζ_{i+1} . This transformation reduces the polynomial structure Eq. (12) to the tabular form presented in Table 1. The quintic Hermite polynomials are presented on the interval $[\zeta_i, \zeta_{i+1}]$ in Table 1 and the values of Hermite splines and its derivatives are presented in Table 2 at $\omega = 0$ and 1. The approximating function at each time level t_{n+1} within each sub-interval is taken as

$$u^{n+1}(\omega) = \sum_{i=1}^6 c_i^{n+1} H_i(\omega); \quad v^{n+1}(\omega) = \sum_{i=1}^6 d_i^{n+1} H_i(\omega). \tag{13}$$

Table 1 Presentation of quintic Hermite splines

i	H_i	H'_i	H''_i
1	$1 - 10\omega^3 + 15\omega^4 - 6\omega^5$	$-30\omega^2 + 60\omega^3 - 30\omega^4$	$-60\omega + 180\omega^2 - 120\omega^3$
2	$h(\omega - 6\omega + 8\omega^4 - 3\omega^5)$	$h(1 - 18\omega^2 + 32\omega^3 - 15\omega^4)$	$h(-36\omega + 96\omega^2 - 60\omega^3)$
3	$\frac{h^2}{2}(\omega^2 - 3\omega^3 + 3\omega^4 - \omega^5)$	$\frac{h^2}{2}(2\omega - 9\omega^2 + 12\omega^3 - 5\omega^4)$	$\frac{h^2}{2}(2 - 18\omega + 36\omega^2 - 20\omega^3)$
4	$\frac{h^2}{2}(\omega^3 - 2\omega^4 + \omega^5)$	$\frac{h^2}{2}(3\omega^2 - 8\omega^3 + 5\omega^4)$	$\frac{h^2}{2}(6\omega - 24\omega^2 + 20\omega^3)$
5	$10\omega^3 - 15\omega^4 + 6\omega^5$	$30\omega^2 - 60\omega^3 + 30\omega^4$	$60\omega - 180\omega^2 + 120\omega^3$
6	$h(-4\omega^3 + 7\omega^4 - 3\omega^5)$	$h(-12\omega^2 + 28\omega^3 - 15\omega^4)$	$h(-24\omega + 84\omega^2 - 60\omega^3)$

Table 2 Value of quintic Hermite splines and corresponding first and second order derivative at boundary points

	$\omega = 0$	$\omega = 1$		$\omega = 0$	$\omega = 1$		$\omega = 0$	$\omega = 1$
H_1	1	0	H'_1	0	0	H''_1	0	0
H_2	0	0	H'_2	h	0	H''_2	0	0
H_3	0	0	H'_3	0	0	H''_3	h^2	0
H_4	0	0	H'_4	0	0	H''_4	0	h^2
H_5	0	1	H'_5	0	0	H''_5	0	0
H_6	0	0	H'_6	0	h	H''_6	0	0

The next step is the choice of collocation points. It plays an important role in Hermite collocation. Zeros of orthogonal polynomials are taken as the collocation points such as Jacobi polynomials. Legendre and Chebyshev polynomials are special cases of Jacobi polynomials. In the present study, zeros of shifted Legendre polynomials have been taken as collocation points.

After semi-discretization of the aforementioned equation for $f(u) = u - u^m$, coupled system of equations on using Eq. (10) in (9) and (8) is defined as:

$$\left\{ \frac{v^{n+1} + v^n}{2} \right\} = - \left\{ \frac{u_{\zeta\zeta}^{n+1} + u_{\zeta\zeta}^n}{2} \right\}, \tag{14}$$

$$u^{n+1} - u^n = \varepsilon \Delta t \left\{ \frac{v_{\zeta\zeta}^{n+1} + v_{\zeta\zeta}^n}{2} \right\} - \Delta t \left\{ \frac{v^{n+1} + v^n}{2} \right\} - \frac{\Delta t}{2} \{ f^{n+1}(u) + f^n(u) \}. \tag{15}$$

The quasi linearisation of $f(u) = u^m - u$ has been taken with Taylor series approximation given in [41, 58] as:

$$\begin{aligned} u^m(t + \Delta t) &= u^m(t) + \Delta t (u^m)_t + \mathcal{O}(\Delta t)^2 \\ &= u^m(t) + \Delta t m u^{m-1} u_t + \mathcal{O}(\Delta t)^2. \end{aligned} \tag{16}$$

Again using finite difference approximation i.e.

$$u(t + \Delta t) = u(t) + \Delta t u_t + \mathcal{O}(\Delta t)^2. \tag{17}$$

This implies,

$$\begin{aligned} \Delta t u_t + \mathcal{O}(\Delta t)^2 &= u(t + \Delta t) - u(t) \\ \implies u^m(t + \Delta t) &= u^m(t) + m u^{m-1} (u(t + \Delta t) - u(t)) + \mathcal{O}(\Delta t)^2. \end{aligned} \tag{18}$$

At $t = t_n$

$$u^m(t_{n+1}) = u^m(t_n) + mu^{m-1}(t_n)u(t_{n+1}) - mu^m(t_n) + \mathcal{O}(\Delta t)^2. \tag{19}$$

Using Eq. (19) omitting the second order truncation term, one gets the following coupled system of equations:

$$v^{n+1} + u_{\zeta\zeta}^{n+1} = -(v^n + u_{\zeta\zeta}^n), \tag{20}$$

$$u^{n+1} - u^n = \varepsilon \Delta t \left(\frac{v_{\zeta\zeta}^{n+1} + v_{\zeta\zeta}^n}{2} \right) - \Delta t \left(\frac{v^{n+1} + v^n}{2} \right) + \Delta t \left(\frac{u^{n+1} + u^n}{2} \right) - \Delta t \left(\frac{mu^{n+1}(u^{m-1})^n - (m-2)(u^m)^n}{2} \right), \tag{21}$$

and rearranging the terms, the following coupled system of equations is obtained:

$$\frac{(v^{n+1} + u_{\zeta\zeta}^{n+1})}{2} = -\frac{(v^n + u_{\zeta\zeta}^n)}{2}, \tag{22}$$

$$u^{n+1} + \frac{\Delta t}{2} \left[-\varepsilon v_{\zeta\zeta}^{n+1} + v^{n+1} - u^{n+1} + mu^{n+1}(u^{m-1})^n \right] = u^n + \frac{\Delta t}{2} [\varepsilon v_{\zeta\zeta}^n - v^n + u^n + (m-2)(u^m)^n]. \tag{23}$$

For space discretization, consider the different approximations u^{n+1} and v^{n+1} for u and v , respectively as: $u^{n+1} = \sum_{i=1}^6 c_i^{n+1} H_i(\omega)$ and $v^{n+1} = \sum_{i=1}^6 d_i^{n+1} H_i(\omega)$, $0 \leq \omega \leq 1$.

The approximate solution lies in each subinterval I_i , of Π , where $H_i(\omega)$ are quintic Hermite splines defined over the interval $[0, 1]$. The system of collocation equations obtained after discretization are explained hereunder:

$$\sum_{i=1}^6 \left\{ c_{4(r-1)+i}^{n+1} \kappa_{ji} + d_{4(r-1)+i}^{n+1} \eta_{ji} \right\} = \sum_{i=1}^6 \left\{ c_{4(r-1)+i}^n v_{ji} + d_{4(r-1)+i}^n \alpha_{ji} \right\}, \tag{24}$$

$$\sum_{i=1}^6 \left\{ c_{4(r-1)+i}^{n+1} \rho_{ji} + d_{4(r-1)+i}^{n+1} \gamma_{ji} \right\} = \sum_{i=1}^6 \left\{ c_{4(r-1)+i}^n \chi_{ji} + d_{4(r-1)+i}^n \lambda_{ji} \right\} + \frac{(m-2)\Delta t}{2} \left[\sum_{i=1}^6 c_{4(r-1)+i}^n H_i(\omega_j) \right]^m, \tag{25}$$

where, $r = 1, 2, 3, \dots, N$. $j = 1, 2, 3, 4$. c_i and d_i are unknown coefficients and the constant parameters are defined as:

$$\begin{aligned} \rho_{ji} &= H_i(\omega_j) - \frac{\Delta t}{2} H_i(\omega_j) + \frac{m\Delta t}{2} H_i(\omega_j) \left\{ \sum_{i=1}^6 c_{4(r-1)+i}^n H_i(\omega_j) \right\}^{m-1}, \\ \lambda_{ji} &= \frac{\varepsilon \Delta t}{2h^2} H_i''(\omega_j) - \frac{\Delta t}{2} H_i(\omega_j), \\ \gamma_{ji} &= \frac{-\varepsilon \Delta t}{2h^2} H_i''(\omega_j) + \frac{\Delta t}{2} H_i(\omega_j); \quad v_{ji} = \frac{-1}{2h^2} H_i''(\omega_j), \\ \chi_{ji} &= H_i(\omega_j) + \frac{\Delta t}{2} H_i(\omega_j); \quad \eta_{ji} = \frac{1}{2} H_i(\omega_j), \\ \kappa_{ji} &= \frac{1}{2h^2} H_i''(\omega_j); \quad \alpha_{ji} = -\frac{1}{2} H_i(\omega_j). \end{aligned} \tag{26}$$

Total number of variables are $8N + 4$ and the collocation equations are $8N$. The extra four variables are computed from the boundary conditions. Again, in compact form, the system of EFK equation can be written as:

$$[\mathbf{L}]y^{n+1} = [\mathbf{J}]y^n + \mathbf{f}^n, \tag{27}$$

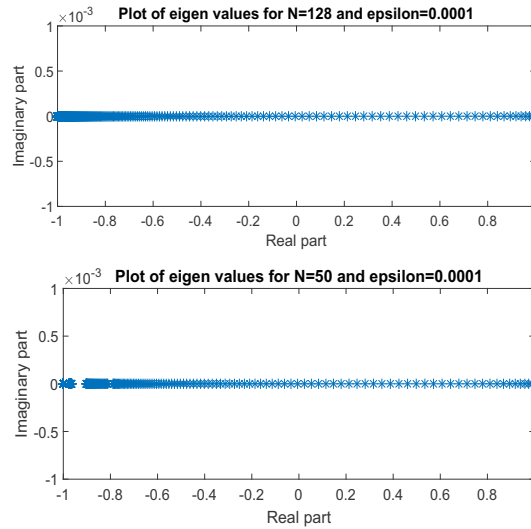


Fig. 1 Behaviour of eigen values at $N = 128$ and $N = 50$ with $\varepsilon = 0.0001$

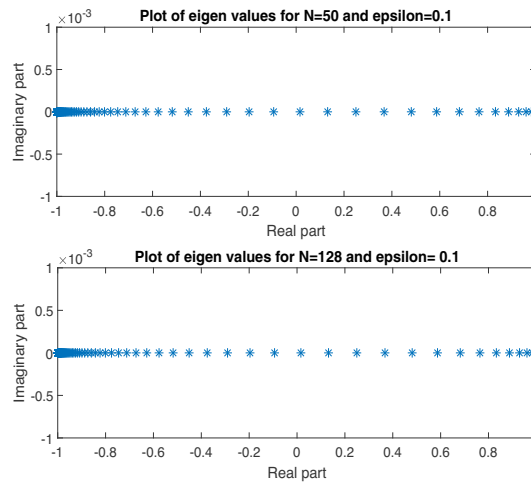


Fig. 2 Behaviour of eigen values at $N = 128$ and $N = 50$ with $\varepsilon = 0.1$

The component matrices \mathbf{L} and \mathbf{J} both depends on the perturbation parameters, grid sizes towards both space and time directions and the Hermite splines adopted for approximation.

Let λ be the eigen value of the matrix $[\mathbf{L}^{-1}\mathbf{J}]$. It is observed computationally that the magnitude of eigen values of matrix $[\mathbf{L}^{-1}\mathbf{J}]$ are bounded by unity. The behaviour of eigenvalues is shown in Figs. 1 and 2 for $N = 128$ and $N = 50$ corresponding to $\varepsilon = 0.0001$ and $\varepsilon = 0.1$, respectively (Fig. 3).

It is observed that the imaginary part of eigen values is zero and the real part of eigen values is less than unity, i.e., $|\lambda| \leq 1$ which signifies the stability of the proposed iterative technique by Lax–Richtmyer definition for stability.

NOTE: u has been considered as locally constant η (say) for the quasi linearization of the non-linear term. The implemented technique comprises both the operators \mathcal{F} and \mathcal{T} operate on both u and v i.e. $\mathcal{F}_{u,v}$ and $\mathcal{T}_{u,v}$ simultaneously and thus approximating two set of values at each iteration at the chosen collocation points for the two approximate solutions \tilde{u} and \tilde{v} . Thus, the iterative scheme at each time step, approximate a function consisting of two component functions u and v i.e. $\mathbf{U} = \{u, v\}$ using the different Hermite interpolating polynomial function i.e. $\mathbf{H} = \{\tilde{H}_1, \tilde{H}_2\}$. Since, u is bounded, hence operators can be linearised by considering η as the maximum bound of $(u^{m-1})^n$, where $(u^{m-1})^n = u(t_n)^{m-1}$

For Crank–Nicolson scheme, the operators are represented as:
 $\mathcal{F}_{u,v}(\omega_i) = P_1(u^j(\omega_i), v^j(\omega_i))$ and $\mathcal{T}_{u,v}(\omega_i) = P_2(u^j(\omega_i), v^j(\omega_i))$,

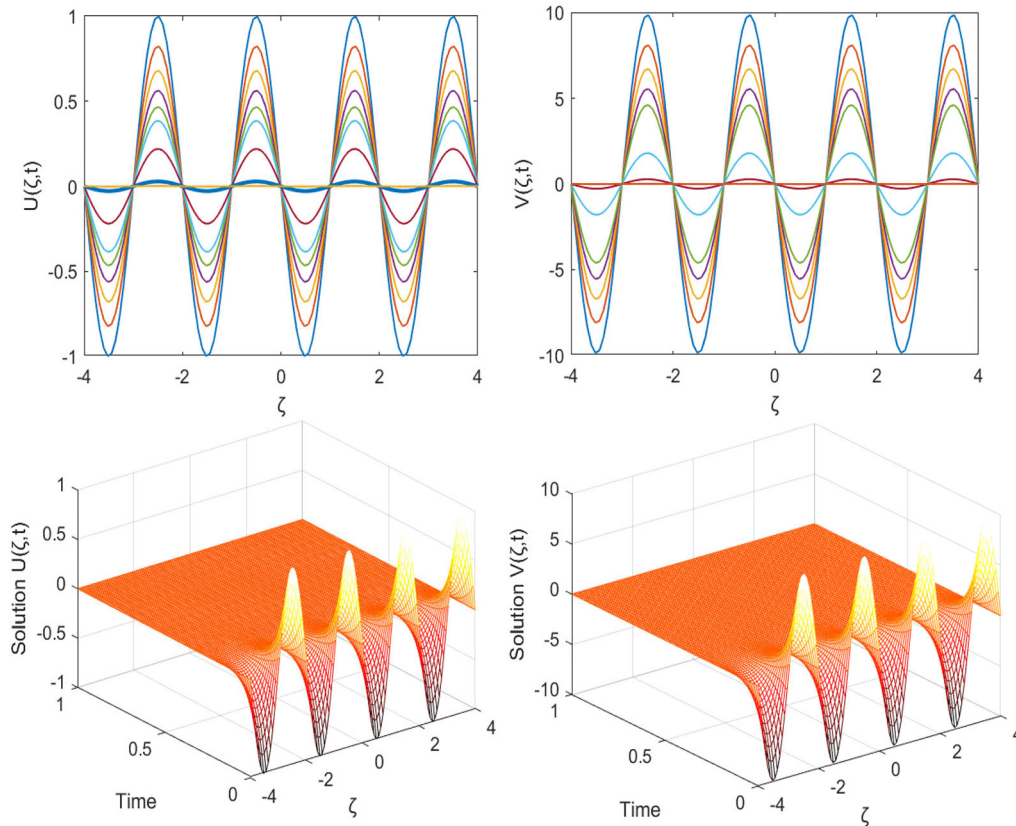


Fig. 3 Behavior of wave solution $u(\zeta, t)$ and absolute error with $N = 50$ and $\Delta t = 0.01$ for Example 6.1

where,

$$\begin{aligned} \mathcal{F}(\mathbf{U}(\omega_i)) &= \mathcal{F}_{u,v}(\omega_i) = v^{j+1}(\omega_i) + u_{\zeta\zeta}^{j+1}(\omega_i), \\ \mathcal{T}(\mathbf{U}(\omega_i)) &= \mathcal{T}_{u,v}(\omega_i) = u^{j+1}(\omega_i) - \frac{\Delta t}{2}(\varepsilon v_{\zeta\zeta}^{j+1}(\omega_i) - v^{j+1}(\omega_i) + (1 - m\eta)u^{j+1}(\omega_i)), \\ P_1(u^j(\omega_i), v^j(\omega_i)) &= -v^j(\omega_i) - u_{\zeta\zeta}^j(\omega_i), \\ P_2(u^j(\omega_i), v^j(\omega_i)) &= u^j(\omega_i) + \frac{\Delta t}{2}(\varepsilon v_{\zeta\zeta}^j(\omega_i) - v^j(\omega_i) + (1 + (m - 2)\eta)u^j(\omega_i)). \end{aligned}$$

The matrix notation for the parameters and collocation equations can be written as:

$$L y^{j+1} = \begin{bmatrix} \mathcal{F}_{u,v} \\ \mathcal{T}_{u,v} \end{bmatrix}, \quad J y^j = \begin{bmatrix} P_1^j \\ P_2^j \end{bmatrix}, \quad y^j = \begin{bmatrix} d_i^j \\ c_i^j \end{bmatrix},$$

where y^j contains the coefficients of Hermite polynomials.

Let $\tilde{\mathbf{U}} = \{\tilde{u}, \tilde{v}\}$ be the approximation of $\mathbf{U} = \{u, v\}$ and $\tilde{\mathbf{H}} = \{\tilde{H}_1, \tilde{H}_2\}$ be the Hermite approximation to the function $\mathbf{U} = \{u, v\}$. These functions have two component functions and are defined on $C^6[a, b]$.

5 Convergence analysis

Lemma 5.1 [17,40] For Crank–Nicolson scheme, local truncation error e_{n+1} estimate and global truncation error E_{n+1} estimate are of $\mathcal{O}(\Delta t)^3$ and $\mathcal{O}(\Delta t)^2$, respectively, i.e.

$$\| e_{n+1} \|_{\infty} \leq C(\Delta t)^3 \quad \text{and} \quad \| E_{n+1} \|_{\infty} \leq C(\Delta t)^2.$$

Theorem 5.2 [40] Let $U(\zeta, t)$ be the function such that $\mathbb{E}U = 0$ and $U \leq C$, C being an arbitrary constant then U_t is also bounded by some constant C .

Lemma 5.3 [61] Let $u(\zeta, 0)$ be the positive continuous initial solution of non-linear reaction–diffusion equation with $0 \leq u(\zeta, 0) \leq 1$ then the bounds for solution $u(\zeta, t)$ remains constant with time.

Through out the paper C denotes the generic constant.

Theorem 5.4 [43] If any Hermite interpolation problem based on at the most two distinct points has a unique solution in Ω then any Hermite interpolation problem has a unique solution in Ω . This implies any Hermite interpolation problem has a unique solution in the polynomial space P_n of degree n on I .

Theorem 5.5 [43] The univariate Hermite interpolating polynomials are regular for any set of nodes. Moreover, Hermite interpolating polynomials are regular for any nodal set as well as for any choice of derivatives to be interpolated.

Theorem 5.6 [43] Let $\bar{\mathcal{H}}$ be the space of all Hermite interpolating polynomials of order 5 defined on $[0, 1]$. Then the Hermite splines of order 5 are bounded with upper bound unity. Moreover, $\sum_{i=1}^6 |H_i(\zeta)| \leq 6$, for all $0 \leq \zeta \leq 1$.

Theorem 5.7 [32,52] Suppose $\mathbf{H} \in H_{\Delta\zeta}^{2q}(\zeta)$ be the piecewise Hermite spline of degree $2q - 1$ over the subinterval $[\zeta_i, \zeta_{i+1}]$ approximating $\mathbf{U} \in C^{2q}[a, b]$ then $\|\mathbf{H}^{(r)} - \mathbf{U}^{(r)}\|_{\infty} \leq O(h^{2q-r})$, $r = 1, 2, \dots, q - 1$.

Proof Let us define a function

$$\bar{H}(\zeta) = \sum_{j=1}^2 u(\zeta_j)\varphi_{j1}(\zeta) + \sum_{j=1}^2 u'(\zeta_j)\varphi_{j2}(\zeta) + \dots + \sum_{j=1}^2 u^{q-1}(\zeta_j)\varphi_{jq}(\zeta), \tag{29}$$

$$\bar{\bar{H}}(\zeta) = \sum_{j=1}^2 v(\zeta_j)\vartheta_{j1}(\zeta) + \sum_{j=1}^2 v'(\zeta_j)\vartheta_{j2}(\zeta) + \dots + \sum_{j=1}^2 v^{q-1}(\zeta_j)\vartheta_{jq}(\zeta), \tag{30}$$

where both the sets $\{\varphi_{ji}(\zeta)\}$ and $\{\vartheta_{ji}(\zeta)\}$ are of total $2q$ polynomial members, each of degree $2q - 1$ satisfying

$$\varphi_{ji}^{(i-1)}(\zeta_k) = \delta_{jk} \quad \text{and} \quad \vartheta_{ji}^{(i-1)}(\zeta_k) = \delta_{jk} \tag{31}$$

where ζ_k is the node point $i = 1, 2, 3, 4, \dots, q$ and at node points $\mathbf{H}(\zeta)$ satisfies

$$\mathbf{H}^{(r)}(\zeta_i) = \mathbf{U}^{(r)}(\zeta_i), \tag{32}$$

for $r = 0, 1, 2, \dots, q - 1$ and $\mathbf{H}^{(r)}(\zeta_i) = \{\bar{H}^{(r)}(\zeta_i), \bar{\bar{H}}^{(r)}(\zeta_i)\}$ and $\mathbf{U}^{(r)}(\zeta_i) = \{u^{(r)}(\zeta_i), v^{(r)}(\zeta_i)\}$ with

$$\bar{H}^r(\zeta_i) = u^r(\zeta_i) \quad \text{and} \quad \bar{\bar{H}}^r(\zeta_i) = v^r(\zeta_i),$$

considering above Eq. (32) and Rolle’s theorem, $\mathbf{H}^{(r)}(\zeta) - \mathbf{U}^{(r)}(\zeta)$ has $r + 2$ zeros in $[\zeta_1, \zeta_2]$

$$\zeta_1 = z_1 \leq z_2 \leq \dots \leq z_{r+1} \leq z_{r+2} = \zeta_2 \quad \text{for } r = 0, 1, \dots, q - 1.$$

Let us define a function $\mathbf{D}(\zeta) = \{D_1(\zeta), D_2(\zeta)\}$ on domain having the collection z'_i ’s glued with ϑ , as its zeroes such that

$$\mathbf{D}(\zeta) = \left[\mathbf{U}^{(r)}(\zeta) - \mathbf{H}^{(r)}(\zeta) \right] - \left[\mathbf{U}^{(r)}(\vartheta) - \mathbf{H}^{(r)}(\vartheta) \right] \frac{\mathbf{S}(\zeta)}{\mathbf{S}(\vartheta)}, \tag{33}$$

for $r = 0, 1, 2, \dots, q - 1$, where $\mathbf{S}(\zeta)$ is defined as a polynomial function of degree $2q - r$ having z'_i ’s as single zeroes except z_1 and z_2 of equal multiplicity and ϑ is any arbitrary point of domain $[\zeta_1, \zeta_2]$ differ from z'_i ’s.

For any r , $\mathbf{D}(\zeta)$ has $r + 3$ zeros, the degree of polynomial $\mathbf{S}(\zeta)$ decreases as r increases.

Combine Eq. (31), Eq. (32) and Rolle’s theorem, it is ready that $(q - r - 1)$ th order derivative of $\mathbf{D}(\zeta)$ has a total of $q + 2$ zeroes.

This assures the existence of a real $\xi \in [a, b]$ (say) such that

$$\mathbf{D}^{(2q-r)}(\xi) = 0, \tag{34}$$

$$\mathbf{U}^{(2q)}(\xi) - \frac{\mathbf{U}^{(r)}(\vartheta) - \mathbf{H}^{(r)}(\vartheta)}{\mathbf{S}(\vartheta)}(2q - r)! = 0, \tag{35}$$

$$\Rightarrow \mathbf{U}^{(r)}(\vartheta) - \mathbf{H}^{(r)}(\vartheta) = \frac{\mathbf{U}^{(2q)}(\xi)}{(2q - r)!}\mathbf{S}(\vartheta), \tag{36}$$

since maximum of $|(\zeta - \zeta_1)(\zeta - \zeta_2)|$ is $(\zeta_2 - \zeta_1)^2/2^2$ and ϑ is arbitrary point in $[\zeta_1, \zeta_2]$, one gets

$$\| \mathbf{U}^{(r)}(\zeta) - \mathbf{H}^{(r)}(\zeta) \|_\infty \leq \alpha_r h^{2q-r}, \tag{37}$$

for $h = \zeta_{i+1} - \zeta_i$ and $\alpha_r = \frac{\|u^{(2q)}(\xi)\|}{2^{2q-r}(2m-r)!}$ $r = 0, 1, 2, \dots, q - 1$ and $[r] = r + 1$ for r odd, otherwise $[r] = r$. □

For $q = 2$ Theorem 5.7 gives error bounds for cubic Hermite splines and for $q = 3$ Theorem 5.7 gives error bounds for quintic Hermite splines.

Theorem 5.8 *Let $\bar{\mathbf{U}}(\zeta)$ be the approximate solution of the function $\mathbf{U}(\zeta)$ defined on $[a, b]$ such that $\mathbf{U}(\zeta) \in C^6[a, b]$ and $\mathbf{H}(\zeta)$ be the quintic Hermite splines interpolate of $\mathbf{U}(\zeta)$. Then the error estimate $\| \mathbf{U} - \bar{\mathbf{U}} \|$ is defined by:*

$$\| \mathbf{U}(\zeta) - \bar{\mathbf{U}}(\zeta) \|_\infty \leq C \left(\alpha_0 h^6 + \max \left\{ h^4(\alpha_2 + \alpha_0 h^2), h^4 \left(\frac{\varepsilon \Delta t \alpha_2}{2} + \frac{\Delta t \alpha_0}{2} h^2 + \left(1 + \frac{\Delta t(1 - \eta m)}{2} \right) \alpha_0 h^2 \right) \right\} \right).$$

Proof Let $\bar{\mathbf{U}}_1(\zeta)$ and $\bar{\mathbf{U}}_2(\zeta)$ be the appropriate approximating functions defined by Theorem 5.4, with $\bar{\mathbf{U}} = \{ \bar{\mathbf{U}}_1, \bar{\mathbf{U}}_2 \}$, corresponding to the uniform grid in space direction with nodal gap h . Let $\mathbf{H}(\zeta) = \{ \bar{\mathbf{H}}(\zeta), \bar{\bar{\mathbf{H}}}(\zeta) \}$ be the quintic Hermite spline approximating $\mathbf{U}(\zeta) = \{ u(\zeta), v(\zeta) \}$. $\bar{\mathbf{H}}(\zeta)$ be the quintic Hermite spline of $u(\zeta)$ and $\bar{\bar{\mathbf{H}}}(\zeta)$ be the quintic Hermite spline of $v(\zeta)$. Now,

$$\| \mathcal{F}\mathbf{U}(\zeta_i) - \mathcal{F}\mathbf{H}(\zeta_i) \|_\infty = \| v(\zeta_i) - \bar{\bar{\mathbf{H}}}(\zeta_i) + u''(\zeta_i) - \bar{\mathbf{H}}''(\zeta_i) \|_\infty, \tag{38}$$

$$\begin{aligned} \| \mathcal{T}\mathbf{U}(\zeta_i) - \mathcal{T}\mathbf{H}(\zeta_i) \|_\infty &= \| (u(\zeta_i) - \bar{\mathbf{H}}(\zeta_i)) - \frac{\varepsilon \Delta t}{2} (v''(\zeta_i) - \bar{\bar{\mathbf{H}}}''(\zeta_i)) \\ &\quad + \frac{\Delta t}{2} (v(\zeta_i) - \bar{\bar{\mathbf{H}}}(\zeta_i)) - \frac{\Delta t(1 - \eta m)}{2} (u(\zeta_i) - \bar{\mathbf{H}}(\zeta_i)) \|_\infty. \end{aligned} \tag{39}$$

Using Theorem 5.7, one gets

$$\begin{aligned} \| \mathcal{F}\mathbf{U}(\zeta_i) - \mathcal{F}\mathbf{H}(\zeta_i) \|_\infty &\leq Ch^6 + Ch^4 \\ &\leq Ch^4(1 + h^2), \end{aligned} \tag{40}$$

and

$$\begin{aligned} \| \mathcal{T}\mathbf{U}(\zeta_i) - \mathcal{T}\mathbf{H}(\zeta_i) \|_\infty &\leq C \left(h^6 + \frac{\varepsilon \Delta t}{2} h^4 + \frac{\Delta t}{2} h^6 + \frac{\Delta t(1 - \eta m)}{2} h^6 \right) \\ &\leq Ch^4 \left(\frac{\varepsilon \Delta t}{2} + \frac{\Delta t}{2} h^2 + \left(1 + \frac{\Delta t(1 - \eta m)}{2} \right) h^2 \right). \end{aligned} \tag{41}$$

Now, consider:

$$\begin{aligned} \| \mathcal{F}\mathbf{H}(\zeta_i) - \mathcal{F}\bar{\mathbf{U}}(\zeta_i) \|_\infty &= \| P_1(\zeta_i) - \mathcal{F}\bar{\mathbf{U}}(\zeta_i) \|_\infty, \\ \| \mathcal{T}\mathbf{H}(\zeta_i) - \mathcal{T}\bar{\mathbf{U}}(\zeta_i) \|_\infty &= \| P_2(\zeta_i) - \mathcal{T}\bar{\mathbf{U}}(\zeta_i) \|_\infty, \end{aligned}$$

where $\mathcal{F}\mathbf{H}(\zeta_i) = P_1(\zeta_i)$ and $\mathcal{T}\mathbf{H}(\zeta_i) = P_2(\zeta_i)$ are the fully discretized explicit form of differential problem mentioned in Sect. 4.

$$\begin{aligned} \|\mathcal{F}\mathbf{H}(\zeta_i) - \mathcal{F}\bar{\mathbf{U}}(\zeta_i)\|_\infty &\leq \|\mathcal{F}\mathbf{U}(\zeta_i) - \mathcal{F}\bar{\mathbf{U}}(\zeta_i)\|_\infty \\ &\leq Ch^4(1+h^2), \\ \|\mathcal{T}\mathbf{H}(\zeta_i) - \mathcal{T}\bar{\mathbf{U}}(\zeta_i)\|_\infty &\leq \|\mathcal{T}\mathbf{U}(\zeta_i) - \mathcal{T}\bar{\mathbf{U}}(\zeta_i)\|_\infty \\ &\leq Ch^4 \left(\frac{\varepsilon\Delta t}{2} + \frac{\Delta t}{2}h^2 + \left(1 + \frac{\Delta t(1-\eta m)}{2}\right)h^2 \right). \end{aligned} \quad (42)$$

Equation (42) has been obtained using the above equation and again, using

$$\mathcal{F}\bar{\mathbf{U}}(\zeta_i) = \hat{P}_1(\zeta_i) \quad \text{and} \quad \mathcal{T}\bar{\mathbf{U}}(\zeta_i) = \hat{P}_2(\zeta_i),$$

its compact matrix representation

$$\mathbf{L}\hat{y}^{n+1} = \mathbf{J}\hat{y}^n + \mathbf{f}^n. \quad (43)$$

This implies, using Eqs. (43) and (27), one gets

$$\begin{aligned} \mathbf{L}[y^{n+1} - \hat{y}^{n+1}] &= \mathbf{J}[y^n - \hat{y}^n], \\ \Rightarrow [y^{n+1} - \hat{y}^{n+1}] &= \mathbf{L}^{-1}\mathbf{J}[y^n - \hat{y}^n]. \end{aligned} \quad (44)$$

Again, \mathbf{L} is non-singular and boundedness of Hermite splines by unity implies that

$$\|\mathbf{L}^{-1}\|_\infty \leq C, \quad (45)$$

where C is some arbitrary constant. Now,

$$\begin{aligned} \|\mathbf{J}(y^n - \hat{y}^n)\|_\infty &\leq \max \left\{ |P_1(\zeta_i) - \hat{P}_1(\zeta_i)|, |P_2(\zeta_i) - \hat{P}_2(\zeta_i)| \right\} \\ &\leq \max \left\{ |\mathcal{F}\mathbf{H}(\zeta_i) - \mathcal{F}\bar{\mathbf{U}}(\zeta_i)|, |\mathcal{T}\mathbf{H}(\zeta_i) - \mathcal{T}\bar{\mathbf{U}}(\zeta_i)| \right\} \\ &\leq C \max \left\{ h^4(1+h^2), h^4 \left(\frac{\varepsilon\Delta t}{2} + \frac{\Delta t}{2}h^2 + \left(1 + \frac{\Delta t(1-\eta m)}{2}\right)h^2 \right) \right\}. \end{aligned} \quad (46)$$

From Eqs. (44), (45) and (46) one derives

$$\|y^{n+1} - \hat{y}^{n+1}\|_\infty \leq C \max \left\{ h^4(1+h^2), h^4 \left(\frac{\varepsilon\Delta t}{2} + \frac{\Delta t}{2}h^2 + \left(1 + \frac{\Delta t(1-\eta m)}{2}\right)h^2 \right) \right\}. \quad (47)$$

Moving towards the error bounds of

$$\begin{aligned} \|\bar{H}(\zeta) - \bar{v}(\zeta)\|_\infty &= \left\| \sum_{i=1}^6 (d_i(t) - \hat{d}_i(t))H_i(\zeta) \right\|_\infty \\ &\leq \sum_{i=1}^6 |H_i(\eta)| \|d_i(t) - \hat{d}_i(t)\|_\infty \\ &\leq Ch^4(\alpha_2 + \alpha_0 h^2). \end{aligned} \quad (48)$$

Equation (48) is obtained using Eq. (47) and boundedness of $H_i(\zeta)$ by 1. Similarly,

$$\begin{aligned} \|\bar{H}(\zeta) - \bar{u}(\zeta)\|_\infty &= \left\| \sum_{i=1}^6 (c_i(t) - \hat{c}_i(t))H_i(\zeta) \right\|_\infty \\ &\leq \sum_{i=1}^6 |H_i(\eta)| \|c_i(t) - \hat{c}_i(t)\|_\infty \\ &\leq Ch^4 \left(\frac{\varepsilon\Delta t\alpha_2}{2} + \frac{\Delta t\alpha_0}{2}h^2 + \left(1 + \frac{\Delta t(1-\eta m)}{2}\right)\alpha_0 h^2 \right). \end{aligned} \quad (49)$$



Combining the above results in Eqs. (48) and (49), one gets

$$\| \mathbf{H}(\zeta) - \bar{\mathbf{U}}(\zeta) \|_{\infty} \leq C \max \left\{ h^4(\alpha_2 + \alpha_0 h^2), h^4 \left(\frac{\varepsilon \Delta t \alpha_2}{2} + \frac{\Delta t \alpha_0}{2} h^2 + \left(1 + \frac{\Delta t(1 - \eta m)}{2} \right) \alpha_0 h^2 \right) \right\}. \tag{50}$$

now,

$$\| \mathbf{U}(\zeta) - \bar{\mathbf{U}}(\zeta) \|_{\infty} \leq \| \mathbf{U}(\zeta) - \mathbf{H}(\zeta) \|_{\infty} + \| \mathbf{H}(\zeta) - \bar{\mathbf{U}}(\zeta) \|_{\infty},$$

using Theorem 5.7 and Eq. (50)

$$\begin{aligned} \| \mathbf{U}(\zeta) - \bar{\mathbf{U}}(\zeta) \|_{\infty} &\leq C \alpha_0 h^6 + C \max \left\{ h^4(\alpha_2 + \alpha_0 h^2), h^4 \left(\frac{\varepsilon \Delta t \alpha_2}{2} + \frac{\Delta t \alpha_0}{2} h^2 + \left(1 + \frac{\Delta t(1 - \eta m)}{2} \right) \alpha_0 h^2 \right) \right\} \\ &\leq C \left(\alpha_0 h^6 + \max \left\{ h^4(\alpha_2 + \alpha_0 h^2), h^4 \left(\frac{\varepsilon \Delta t \alpha_2}{2} + \frac{\Delta t \alpha_0}{2} h^2 + \left(1 + \frac{\Delta t(1 - \eta m)}{2} \right) \alpha_0 h^2 \right) \right\} \right). \end{aligned} \tag{51}$$

□

Theorem 5.9 Let $\bar{\mathbf{U}}(\zeta, t)$ be the approximate solution of the function $\mathbf{U}(\zeta, t)$ defined on $[a, b] \times (0, T]$ such that $\mathbf{U}(\zeta, t) \in C^6[a, b]$ and $\mathbf{H}(\zeta)$ be the quintic Hermite splines interpolate of $\mathbf{U}(\zeta, t)$ with Crank Nicolson scheme in time direction. Then the error estimate $\| \mathbf{U} - \bar{\mathbf{U}} \|_{\infty}$ is defined by:

$$\| \mathbf{U} - \bar{\mathbf{U}} \|_{\infty} \leq C \left((\Delta t)^2 + \alpha_0 h^6 + \max \left\{ h^4(\alpha_2 + \alpha_0 h^2), h^4 \left(\frac{\varepsilon \Delta t \alpha_2}{2} + \frac{\Delta t \alpha_0}{2} h^2 + \left(1 + \frac{\Delta t(1 - \eta m)}{2} \right) \alpha_0 h^2 \right) \right\} \right).$$

Proof Directly from Theorem 5.8 and Lemma 5.1.

□

Parameter uniform rate of convergence

For the problems, where exact solution not known, nodal error is estimated by using the following formula:

$$e_{\varepsilon}^{N,M}(i, m) = | U^{N,M}(i, m) - U^{2N,M}(i, m) |.$$

Maximum nodal error has been calculated by

$$E_{\varepsilon,N,M} = \max_i e_{\varepsilon}^{N,M}(i, m).$$

Maximum ε —uniform nodal error has been calculated by

$$E_{N,M} = \max_{\varepsilon} E_{\varepsilon,N,M},$$

And the parameter ε —uniform rate of convergence has been evaluated by using double mesh principle [45]

$$R_N = \frac{\log(E_{N,M}) - \log(E_{2N,M})}{\log(2)}.$$

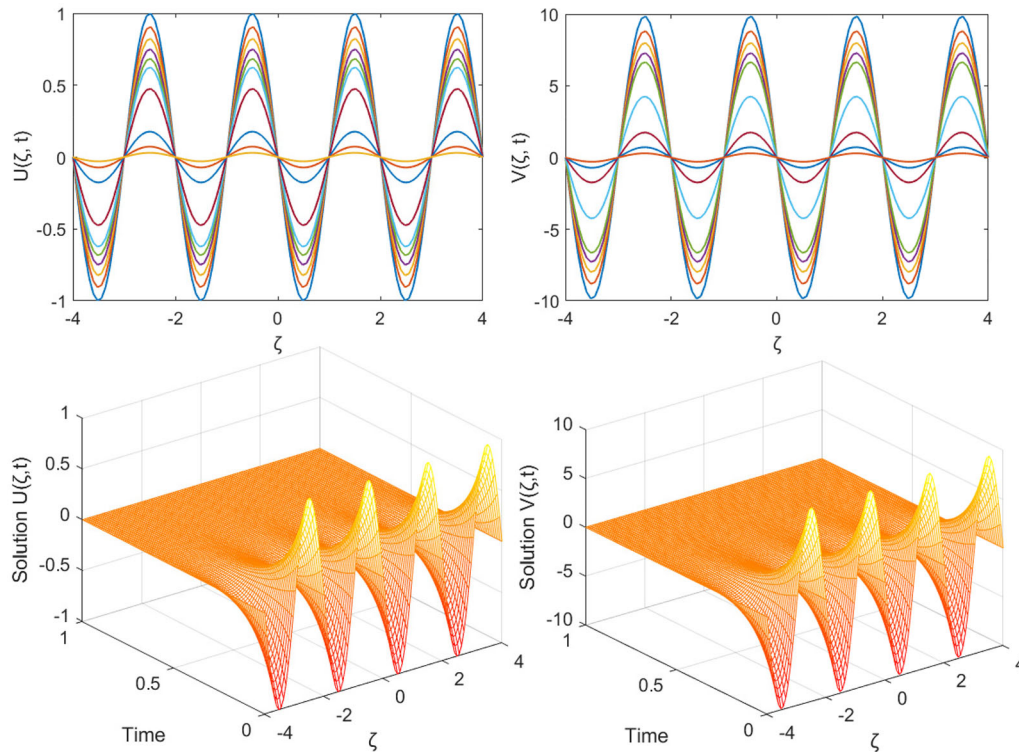


Fig. 4 Behavior of wave solution $u(\zeta, t)$ and $v(\zeta, t)$ with $\varepsilon = 10^{-1}$ for Example 6.1

6 Results and discussion

In this part of manuscript, various fourth order EFK type equation with different non-linear function $f(u)$ has been investigated by the proposed technique. Solution behaviour has been analysed with respect to the different parameters of the technique and the perturbation parameter. The numerical results are presented in the form of graphs and tables. L_2 - norm, L_∞ -norm and Global relative error (GRE) has been computed as-

$$\begin{aligned}
 \| u \|_2 &= \sqrt{h^2 \sum_{j=1}^N u^2(\zeta_j, t)}, \\
 \| u \|_\infty &= \max_i u(\zeta_i, t), \\
 GRE &= \frac{\sum_{j=1}^N | u(\zeta_j, t) - \tilde{u}(\zeta_j, t) |}{\sum_{i=1}^N | u(\zeta_i, t) |}, \tag{52}
 \end{aligned}$$

where $u(\zeta, t)$ denotes the approximate solution and $\tilde{u}(\zeta, t)$ denotes the analytic solution. For computation of L_2 -norm and L_∞ -norm for error, function $u(\zeta, t)$ has been replaced by the error.

Example 6.1 Consider the EFK equation with initial and the boundary conditions defined as:

$$\begin{aligned}
 u(\zeta, 0) &= -\sin(\pi\zeta) \quad x \in [-4, 4], \\
 u(-4, t) &= 0, \quad u(4, t) = 0, \\
 u_{\zeta\zeta}(-4, t) &= 0, \quad u_{\zeta\zeta}(4, t) = 0.
 \end{aligned}$$

The problem has been analyzed for two cases, first when the equation is homogenous and second when it has a non-homogenous part

$f(\zeta, t) = \exp(-t)\sin(\pi\zeta)(\exp(-2t)\sin^2(\pi\zeta) + \pi^2 + \pi^4 - 2)$. For non-homogenous case i.e. $f(\zeta, t) \neq 0$ perturbation parameter $\varepsilon = 1$ has been considered.

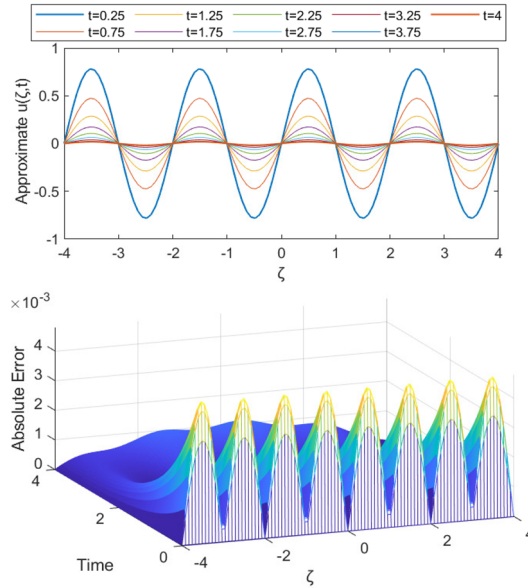


Fig. 5 Behavior of wave solution $u(\zeta, t)$, $v(\zeta, t)$ with $\varepsilon = 10^{-4}$ for Example 6.1

Table 3 Parameter uniform convergence rate at $T = 0.2$ for Example 6.1

ϵ	$N = 16$	$N = 32$	$N = 64$	$N = 128$
2^{-3}	0.00083164	0.00042031	0.000211041	0.000105585
2^{-5}	0.005066764	0.002564092	0.00128547	0.000643064
2^{-6}	0.006815595	0.00345487	0.001732069	0.000866521
2^{-7}	0.007891508	0.004007425	0.002009494	0.001005345
2^{-8}	0.008484801	0.004314483	0.002164167	0.001082758
2^{-9}	0.008795733	0.004475655	0.00224579	0.001123657
2^{-10}	0.008693113	0.004361217	0.002182505	0.00109149
2^{-11}	0.009036136	0.004599197	0.002308712	0.001155332
2^{-12}	0.009076983	0.004620009	0.002319244	0.001160679
2^{-15}	0.009112922	0.004638374	0.002328442	0.00116533
2^{-16}	0.009115493	0.004639694	0.002329104	0.001165659
2^{-17}	0.009116779	0.004640354	0.002329435	0.001165824
E_n	0.009116779	0.004640354	0.002329435	0.001165824
R_N	0.974289335	0.994254794	0.998630068	—

Table 4 Comparison of L_2 , L_∞ and GRE norm due to $\Delta t = 0.01$ and $\Delta t = 0.001$ for Example 6.1 with $N = 64$

Time	$\Delta t = 0.01$			$\Delta t = 0.001$		
	L_2 -norm	L_∞ -norm	GRE	L_2 -norm	L_∞ -norm	GRE
0.0	1.42874e-17	8.88178e-16	3.56768e-09	1.42874e-17	8.88178e-16	3.56768e-09
0.5	8.24109e-05	3.12068e-03	5.01495e-03	6.17258e-06	3.92776e-04	5.14833e-04
1.0	4.84202e-05	1.99664e-03	5.05022e-03	2.17706e-06	3.42516e-04	6.00652e-04
1.5	2.76149e-05	1.34984e-03	5.14661e-03	4.41442e-07	3.47012e-04	1.23549e-03
2.0	1.46576e-05	1.01352e-03	5.53307e-03	2.36769e-06	4.06579e-04	3.32529e-03
2.5	6.26190e-06	9.56217e-04	9.09238e-03	4.07361e-06	5.87362e-04	8.69122e-03
3.0	3.44444e-07	1.17377e-03	2.22965e-02	5.93443e-06	9.52380e-04	2.23252e-02
3.5	4.49788e-06	1.65753e-03	5.66291e-02	8.31754e-06	1.53108e-03	5.67165e-02
4.0	9.32854e-06	2.48154e-03	1.42831e-01	1.16591e-05	2.42139e-03	1.43048e-01

Table 5 Comparison of L_2 -norm L_∞ -norm and GRE with respect to partitions in space and time directions for Example 6.1 at $T = 2$

Time		$N = 20$	$N = 40$	$N = 60$	$N = 80$
$\Delta t = 0.1$	L_2 -norm	1.37406e-03	4.45938e-04	2.08576e-04	1.19453e-04
	L_∞ -norm	8.74229e-03	7.47418e-03	7.10195e-03	6.94779e-03
	GRE	5.28462e-02	5.12724e-02	4.99799e-02	4.99747e-02
$\Delta t = 0.01$	L_2 -norm	1.41692e-04	2.13303e-05	1.60035e-05	7.28243e-05
	L_∞ -norm	2.89695e-03	1.47745e-03	1.05749e-03	4.13368e-03
	GRE	1.90780e-02	8.24560e-03	5.62795e-03	5.00313e-03
$\Delta t = 0.001$	L_2 -norm	1.39713e-04	2.12319e-05	3.32691e-06	5.62754e-07
	L_∞ -norm	6.28584e-04	8.76524e-04	4.51042e-04	2.87972e-04
	GRE	5.35450e-04	7.92931e-03	3.71863e-03	2.16258e-03

Table 6 Comparison of L_∞ -norm with the results with EFG method for Example 6.1

Method		EFGM		QHSCM	
Time		$\Delta t = 0.01$	$\Delta t = 0.001$	$\Delta t = 0.01$	$\Delta t = 0.001$
$T = 1$	$h = 1/10$	7.7195×10^{-2}	2.1542×10^{-2}	2.57163e-03	9.59093e-04
	$h = 1/20$	2.1536×10^{-2}	5.8138×10^{-3}	2.18962e-03	5.45979e-04
	$h = 1/40$	5.8078×10^{-3}	1.4625×10^{-3}	2.01533e-03	3.62735e-04
	$h = 1/80$	1.4567×10^{-3}	3.6573×10^{-4}	1.94303e-03	2.88109e-04
$T = 2$	$h = 1/2.5$	2.8445×10^{-2}	2.8442×10^{-3}	2.89695e-03	6.28584e-04
	$h = 1/5.0$	7.9425×10^{-3}	7.9380×10^{-4}	1.47745e-03	8.76524e-04
	$h = 1/7.5$	2.1437×10^{-3}	2.1386×10^{-4}	1.05749e-03	4.51042e-04
	$h = 1/10$	5.3904×10^{-4}	5.3377×10^{-5}	4.13368e-03	2.87972e-04

Table 7 Comparison of absolute error at different values of ζ for Example 6.1 with $\Delta t = 0.01$ and $N = 64$

Time	$\zeta = -3$	$\zeta = -2$	$\zeta = -1$	$\zeta = 0$	$\zeta = 1$	$\zeta = 2$	$\zeta = 3$
0.0	0.00000e+00	2.22045e-16	0.00000e+00	2.08167e-17	3.33067e-16	1.11022e-16	0.00000e+00
0.5	2.13925e-03	3.11837e-03	2.30463e-03	1.88514e-04	1.98467e-03	2.94162e-03	2.12575e-03
1.0	1.33606e-03	1.95872e-03	1.48480e-03	2.13110e-04	1.09949e-03	1.67968e-03	1.18862e-03
1.5	8.54182e-04	1.26644e-03	1.00450e-03	2.51032e-04	5.33624e-04	8.79348e-04	5.79580e-04
2.0	5.70992e-04	8.65117e-04	7.41180e-04	3.11357e-04	1.43989e-04	3.38703e-04	1.46587e-04
2.5	4.13573e-04	6.50847e-04	6.25200e-04	4.05935e-04	1.64116e-04	7.41854e-05	2.13465e-04
3.0	3.40134e-04	5.65588e-04	6.21818e-04	5.51928e-04	4.60480e-04	4.53962e-04	5.79854e-04

In first case, $\Delta t = 0.01$ and $N = 100$. which is quite less than as considered in [7] with ε is taken to be 0.0001 and 0.1. Numerical profile of $u(\zeta, t)$ and $v(\zeta, t)$ has been shown graphically in Figs. 3 and 4 for $\varepsilon = 0.1$ and 0.0001 respectively. Stable solution profile of EFK is shown for both $\varepsilon = 0.0001$ and $\varepsilon = 0.1$. The solution $u(\zeta, t)$ moves to zero at 40th time step with $\Delta t = 0.01$. The effect of perturbation parameter has been studied and shown in Table 3.

In second case, the analytic form of solution is $u(\zeta, t) = \exp(-t)\sin(\pi\zeta)$ and the initial function has been taken as $u(\zeta, 0) = \sin(\pi\zeta)$. The solution behaviour and the error profile has been depicted in the Fig. 5. The non-homogenous part delays the stable state value in comparison to the homogenous case. L_2 -norm, L_∞ -norm and GRE at different time level with respect to $\Delta t = 0.01$ and $\Delta t = 0.001$ has been reported in Table 4. The effect of Δt and h on L_2 -norm, L_∞ -norm and GRE has been studied in Table 5. At different time level, step size and Δt , a comparison of L_∞ -norm has been given in Table 6 with the results available in [3]. Again the behaviour of absolute error at some node points corresponding to different time levels has been reported in Table 7.

Example 6.2 Consider EFK equation with Gaussian initial condition

$$\begin{aligned}
 \text{(a) } & u(\zeta, 0) = 10^{-3} \exp(-\zeta^2) \quad \zeta \in [-a, a] \text{ with boundary conditions} \\
 & u(-a, t) = 1 \quad u(a, t) = 1, \\
 & u_{\zeta\zeta}(-a, t) = 0 \quad u_{\zeta\zeta}(a, t) = 0.
 \end{aligned}$$



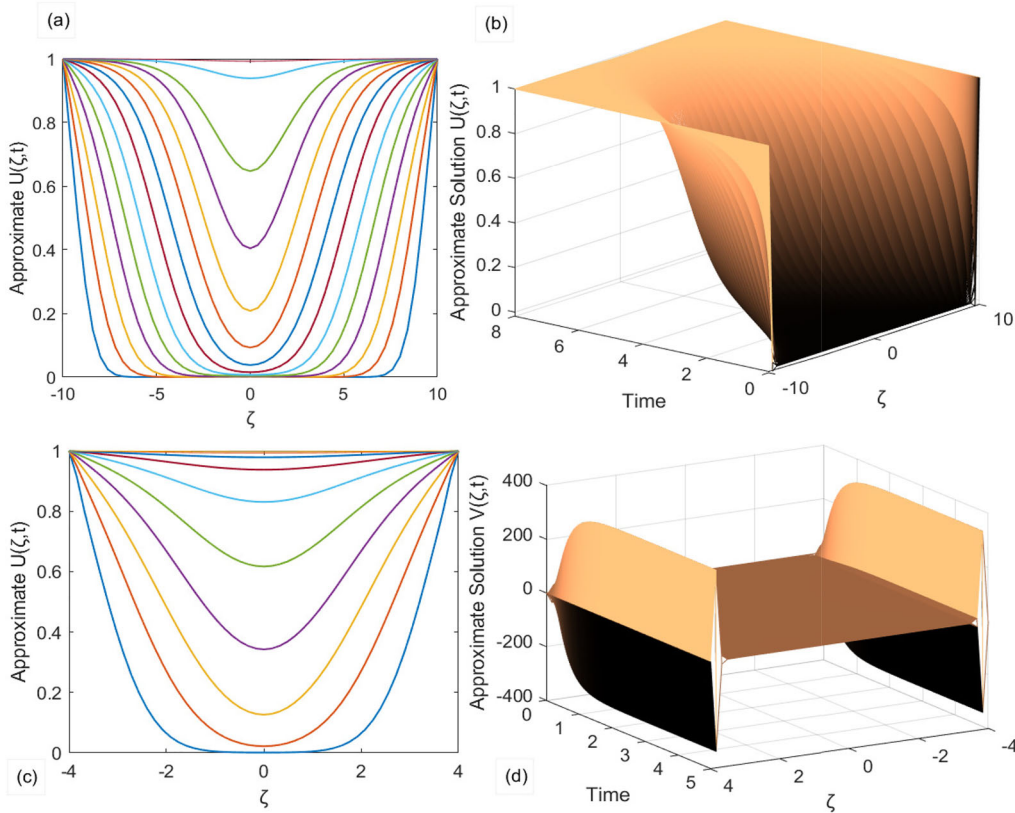


Fig. 6 Stable behavior of solution $u(\zeta, t)$, $v(\zeta, t)$ for Gaussian initial function for Example 6.2(a)

Table 8 Effects on the norms due to domain for Example 6.2(a) with $\Delta t = 0.01$ and $N = 50$ and $\varepsilon = 0.0001$

Time	$\Omega = [-4, 4]$		$\Omega = [-10, 10]$	
	L_2 -norm	L_∞ -norm	L_2 -norm	L_∞ -norm
0.0	5.62590e-02	9.96992e-01	1.40648e-01	9.96992e-01
1.0	1.28174e-01	9.55642e-01	2.93265e-01	8.68283e-01
2.0	1.32535e-01	9.80254e-01	3.21779e-01	9.51480e-01
3.0	1.34241e-01	9.93923e-01	3.32150e-01	9.82345e-01
4.0	1.34822e-01	9.98877e-01	3.35790e-01	9.94613e-01
5.0	1.34938e-01	9.99848e-01	3.36935e-01	9.98470e-01

(b) $u(\zeta, 0) = -10^{-3} \exp(-\zeta^2)$ $\zeta \in [-a, a]$ and boundary conditions
 $u(-a, t) = -1$ $u(a, t) = -1$,
 $u_{\zeta\zeta}(-a, t) = 0$ $u_{\zeta\zeta}(a, t) = 0$.

For case (a), computations for $\Delta t = 0.01$, $N = 50$, and $\varepsilon = 0.0001$ has been considered. Corresponding to different time steps, up-to $T = 5$, for the domain $[-4, 4]$ and up to $T = 8$ for the spatial domain $[-10, 10]$, the numerical profiles are shown in Fig. 6. With the passage of time, the solution decays to the stable state boundary value 1. With the change in domain from $[-4, 4]$ to $[-10, 10]$, the behaviour of $u(\zeta, t)$ delays in the stable state value 1 with increments in the path length for the solution waves at different time. When the initial function is $u(\zeta, 0) = \exp(-\zeta^2)$ the solution moves to the stable state faster.

Case(b) In this case, $\Delta t = 0.01$, $N = 50$ and $\varepsilon = 0.0001$ has been taken. Corresponding to different values of time, up-to $T = 5$ for the domain $[-4, 4]$ and up to $T = 8$ for the domain $[-10, 10]$, the behavior of computed values at the node points has been shown in Fig. 7. In this case also, the solution moves towards the stable state boundary value -1 as the time progresses. For both the cases Examples 6.2(a) and 6.2(b) with change

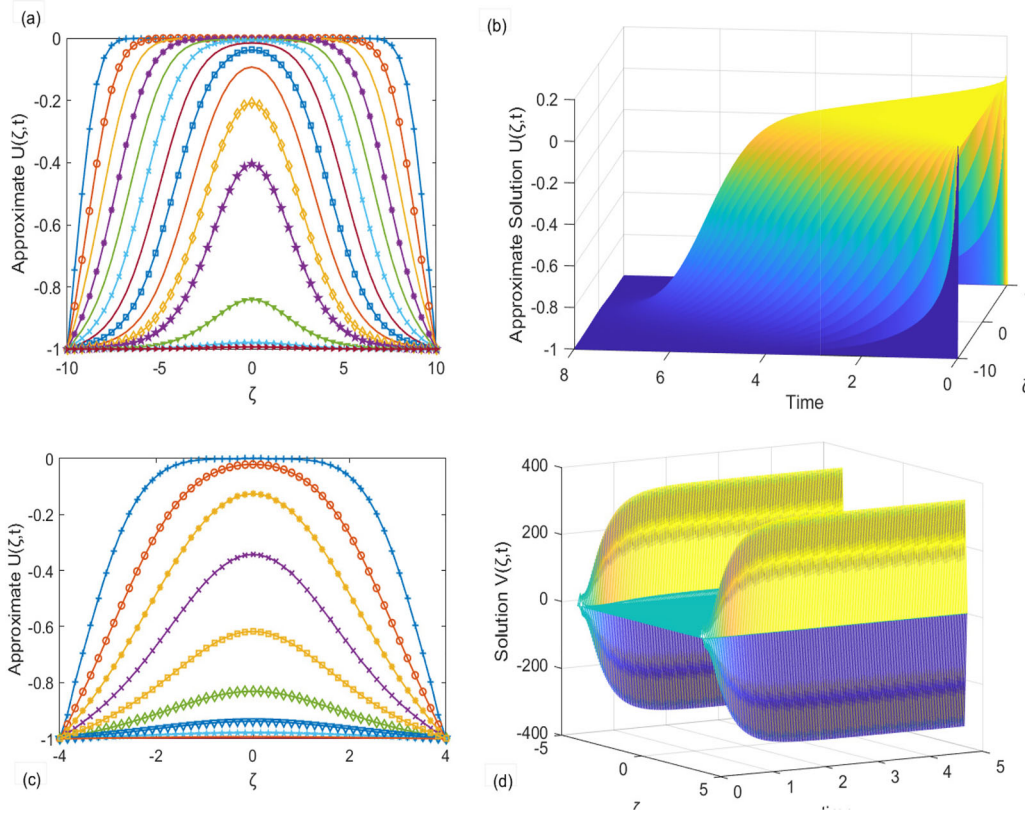


Fig. 7 Behavior of solution $u(\zeta, t)$, $v(\zeta, t)$ for Example 6.2(b)

Table 9 Effects on the norms due to domain for Example 6.2(b) with $\Delta t = 0.01$ and $N = 64$ and $\varepsilon = 0.01$

Time	$\Omega = [-4, 4]$		$\Omega = [-10, 10]$	
	L_2 -norm	L_∞ -norm	L_2 -norm	L_∞ -norm
0.0	4.39524e-02	9.96992e-01	1.09881e-01	9.96992e-01
1.0	1.03420e-01	9.48203e-01	2.38273e-01	9.27997e-01
2.0	1.03640e-01	9.81968e-01	2.55112e-01	9.85379e-01
3.0	1.04187e-01	1.00231e+00	2.60960e-01	9.98986e-01
4.0	1.04572e-01	1.00737e+00	2.62897e-01	1.00066e+00
5.0	1.04813e-01	1.00650e+00	2.63448e-01	9.99607e-01

in domain, L_2 -norm gets effected as compared to L_∞ -norm signifying the delay in stable state as shown in Tables 8 and 9.

Example 6.3 Consider the Eq. (1) for non-linear function $f(u)$ as Fisher’s reaction–diffusion type function:

$$u_t + \varepsilon u_{\zeta\zeta\zeta\zeta} - u_{\zeta\zeta} + u^2 - u = 0 \quad (\zeta, t) \in [-4, 4] \times (0, T], \tag{53}$$

with initial and boundary conditions $u(\zeta, 0) = (1 + \exp(\frac{\zeta}{\sqrt{6}}))^{-2}$,

$$\begin{aligned} u(0, t) &= \left(1 + \exp\left(\frac{(-5t)}{\sqrt{6}}\right)\right)^{-2}, & u(1, t) &= \left(1 + \exp\left(\frac{(1-5t)}{\sqrt{6}}\right)\right)^{-2}, \\ u_{\zeta\zeta}(0, t) &= 0, & u_{\zeta\zeta}(1, t) &= 0. \end{aligned}$$

With $\Delta t = 0.01$ up to $t = 5$ and $N = 50$. It has been observed that for different values of perturbation parameter the solution wave profile remained same. Corresponding to the different bounded domains with $\varepsilon = 1$ the computed solution has been reported in Fig. 8. It is observed that for the domain $[-4, 4]$, the solution

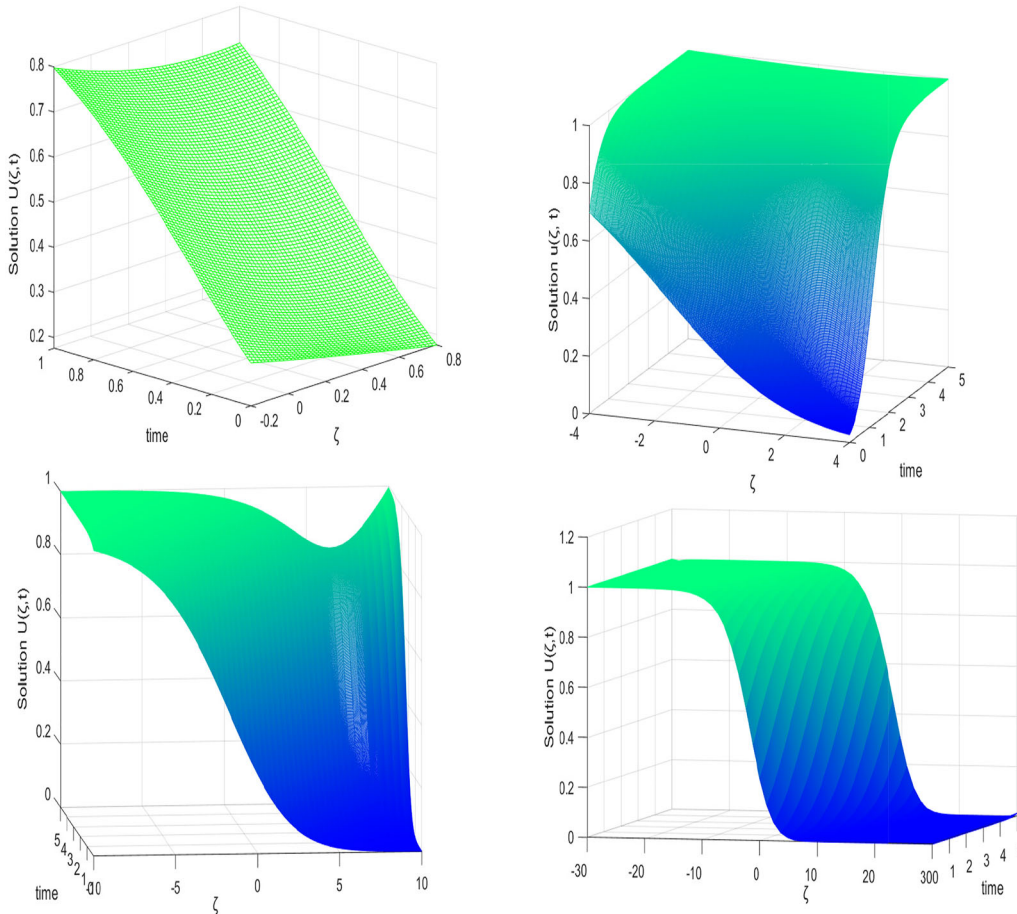


Fig. 8 Behavior of solution profile $u(\zeta, t)$ for Example 6.3 for $\varepsilon = 1$ corresponding to different domain

Table 10 Variations in L_2 -norm and L_∞ -norm due to domain for Example 6.3 with $\Delta t=0.01$ and $N = 64$ and $\varepsilon = 0.01$

Time	$\Omega = [-4, 4]$		$\Omega = [-10, 10]$		$\Omega = [-30, 30]$	
	L_2 -norm	L_∞ -norm	L_2 -norm	L_∞ -norm	L_2 -norm	L_∞ -norm
0.0	3.05161e-03	6.87209e-01	9.18392e-05	9.62431e-01	3.72923e-11	9.99986e-01
1.0	3.50404e-02	9.31452e-01	2.32795e-03	9.89406e-01	3.48395e-10	9.99968e-01
2.0	8.60787e-02	9.84613e-01	4.66779e-02	9.96130e-01	1.37028e-08	9.99973e-01
3.0	1.01901e-01	9.95334e-01	1.74040e-01	9.97860e-01	7.79145e-07	9.99982e-01
4.0	1.04762e-01	9.98226e-01	2.37816e-01	9.98421e-01	4.49760e-05	9.99989e-01
5.0	1.05277e-01	9.99239e-01	2.55671e-01	9.98918e-01	2.25922e-03	9.99993e-01

approaches the stable state and attains stable value 1. For the domain $[-10, 10]$ an uplifting wave at right boundary has been observed within same time range. While for the domain $[-30, 30]$, the solution behaviour is wavy like a fluid falling down an inclined plane. The effect of domain on the wave behaviour at any time can also be observed from L_2 -norm and L_∞ -norm along the row in Table 10.

Example 6.4 Consider the EFK equation

$$u_t + \varepsilon u_{\zeta\zeta\zeta\zeta} - u_{\zeta\zeta} + u^3 - u = 0 \quad (\zeta, t) \in [0, 1] \times (0, T], \tag{54}$$

with initial and boundary conditions are defined as:

$$\begin{aligned} \text{(a) } u(\zeta, 0) &= \zeta^2(1 - \zeta)^2, & \text{(b) } u(\zeta, 0) &= \zeta^3(1 - \zeta)^3, \\ u(0, t) &= 0 & u(1, t) &= 0, \\ u_{\zeta\zeta}(0, t) &= 0 & u_{\zeta\zeta}(1, t) &= 0. \end{aligned}$$

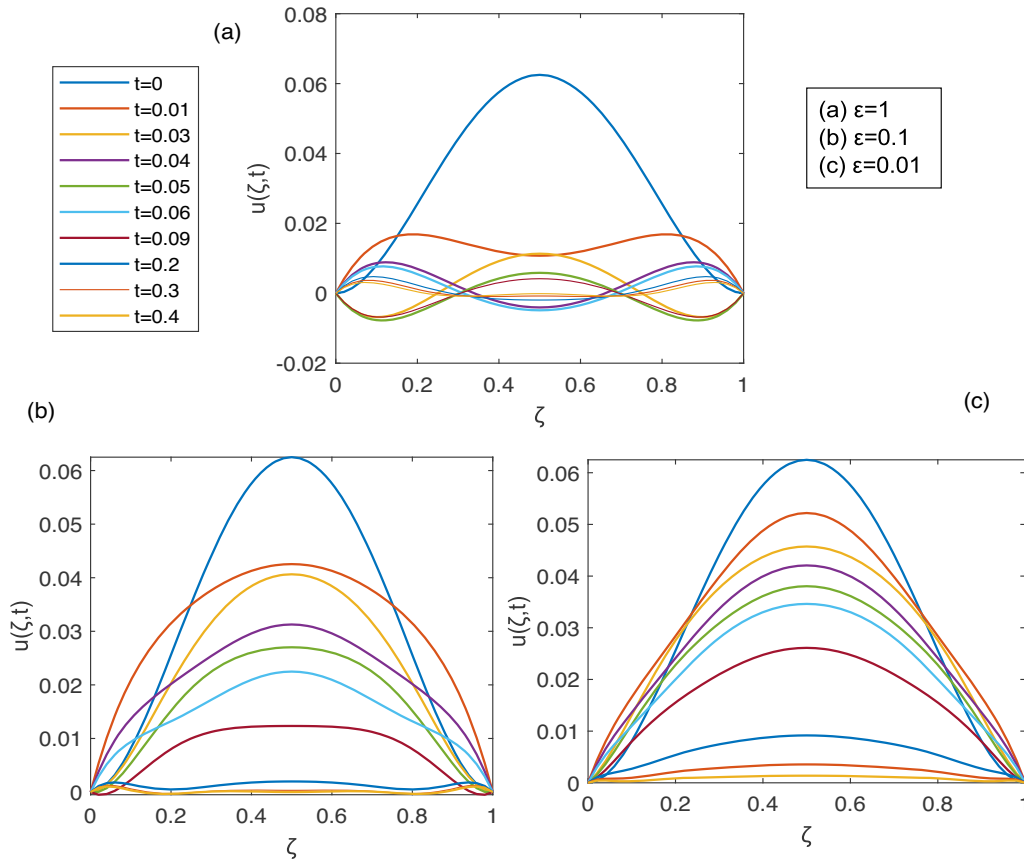


Fig. 9 Behavior of solution profile $u(\zeta, t)$ for Example 6.4(a) for different ε

Table 11 Presentation of L_2 -norm and L_∞ -norm with $\Delta t = 0.01$ and $N = 50$ for Example 6.4

Time	$\varepsilon = 1$		$\varepsilon = 0.001$	
	L_2 -norm	L_∞ -norm	L_2 -norm	L_∞ -norm
0.00	1.06747e-07	1.56246e-02	1.06747e-07	1.56246e-02
0.03	1.02705e-05	4.03076e-03	8.83277e-06	1.08170e-02
0.05	1.04213e-05	2.90052e-03	8.43253e-06	8.73905e-03
0.07	9.69180e-06	2.67816e-03	7.19451e-06	7.26425e-03
0.1	8.26858e-06	2.22327e-03	5.05261e-06	5.06879e-03
0.3	4.11284e-06	9.31101e-04	8.30286e-07	8.42396e-04
0.5	2.49526e-06	4.75279e-04	1.29601e-07	1.40001e-04
0.7	1.81930e-06	3.07393e-04	1.54302e-08	2.32675e-05
0.8	1.63271e-06	2.65424e-04	2.93852e-09	9.48525e-06
0.9	1.49806e-06	2.36168e-04	2.60093e-09	3.86667e-06
1.0	1.39612e-06	2.15282e-04	4.04688e-09	1.57621e-06

With $\Delta t = 0.01$, $N = 50$ and $\varepsilon = 0.01, 0.1$ and 1 . For initial condition (a) the behaviour of solution profile corresponding to different time steps and different values of ε has been shown in Fig. 9. For initial condition (b) with $\varepsilon = 0.1$ and with $\varepsilon = 0.01$ the behavior of solution profile $u(\zeta, t)$ and $v(\zeta, t)$ corresponding to different time steps has been shown in Fig. 10a, b, c and d, respectively.

For $\varepsilon = 0.01$ the solution profile moves to stable state value uniformly, but with a slight increment in the value of perturbation parameter the solution approaches to its stable state with alternating waves having different amplitudes, one with a slight oscillation. Further, when $\varepsilon = 1$, the stable state value has been attained but again the waves' behaviour is alternating, one oscillatory wave with above the stable state and another oscillatory wave below the stable state value. It is observed from the Table 11 that the perturbation parameter effects the nature of waves as compared to the technique parameters for both space and time discretization.

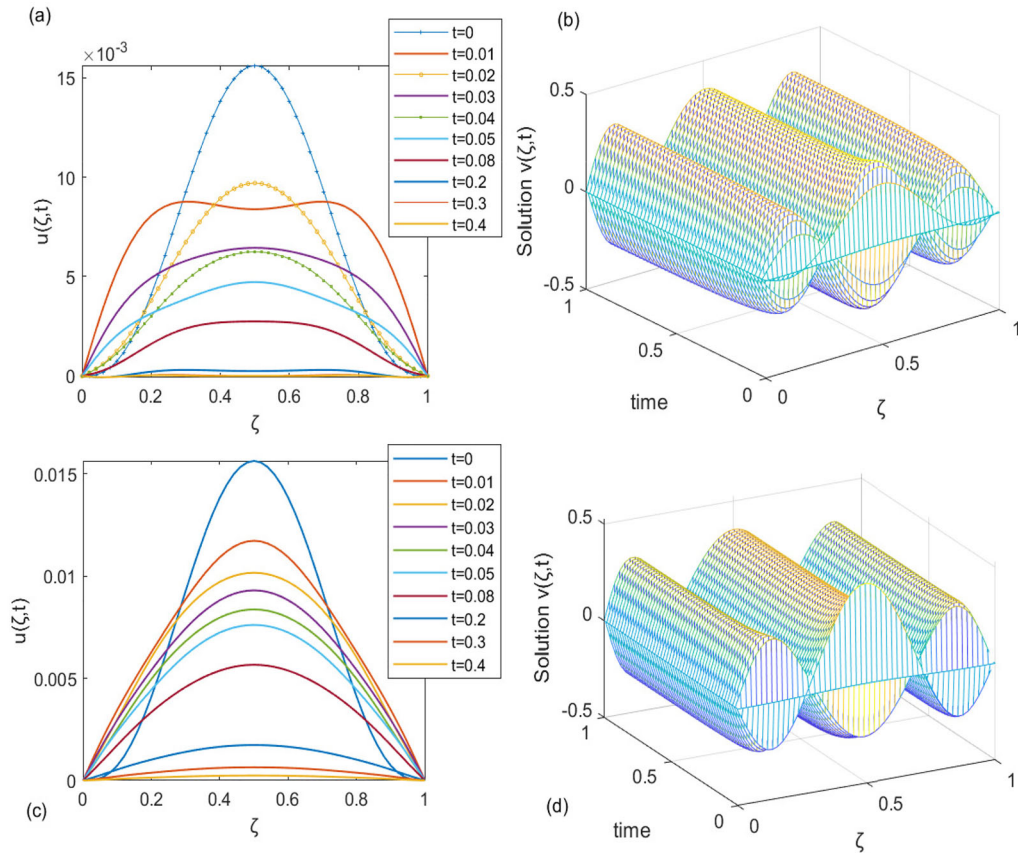


Fig. 10 Behavior of solution $u(\zeta, t)$ and $v(\zeta, t)$ for $\varepsilon = 0.1$ and 0.01 for Example 6.4(b)

Table 12 Parameter uniform convergence rate at $T = 0.04$ for Example 6.4

ε	$N = 8$	$N = 16$	$N = 32$	$N = 64$
2^0	6.41841E-06	3.22272E-06	1.60909E-06	8.03679E-07
2^{-1}	1.80796E-05	8.98549E-06	4.68089E-06	2.34057E-06
2^{-2}	0.00010412	0.00005501	2.78666E-05	1.39476E-05
2^{-3}	6.41841E-06	3.22272E-06	1.60909E-06	8.05E-07
2^{-4}	8.66285E-05	4.60583E-05	2.31932E-05	1.15962E-05
2^{-6}	0.00010412	0.00005501	2.78666E-05	1.39476E-05
2^{-8}	0.00010412	0.00005501	2.78666E-05	1.39476E-05
E_n	0.00010412	0.00005501	2.78666E-05	1.39476E-05
R_n	0.920481409	0.981156913	0.998520095	-

Parameter uniform rate of convergence of order one for Example 6.4(b) has been reported in Table 12 with $\Delta t = 10^{-3}$.

Example 6.5 Consider the fourth order differential equation

$$u_t + \gamma u_{\zeta\zeta\zeta\zeta} - u_{\zeta\zeta} = \alpha u^5 + \beta u^3 + \kappa u^2 \quad (\zeta, t) \in [a, b] \times [0, T], \tag{55}$$

For $\alpha = 24$, $\beta = -2$ and $\kappa = -2$ and $\gamma = 1$ the exact form of solution of Eq. (55) is

$$u(\zeta, t) = \frac{1}{\zeta + 2t} \quad (\zeta, t) \in [a, b] \times [0, T]. \tag{56}$$

The absolute error has been shown in Fig. 11. There is no major improvement in the error as time step decreases from $\Delta t = 0.01$ to $\Delta t = 0.001$ with $N = 50$ as in Table 13. The effect of time on the L_2 norm

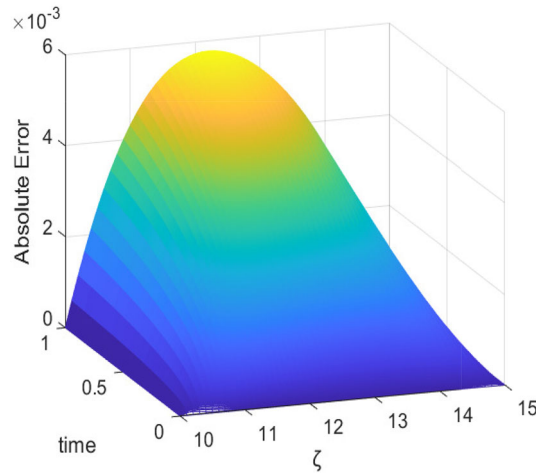


Fig. 11 Absolute error profile of Example 6.5

Table 13 L_2 -norm and L_∞ -norm for error at $\Delta t = 0.01$ and $\Delta t = 0.001$ for Example 6.5

Time	$\Delta t = 0.01$		$\Delta t = 0.001$	
	L_2 -norm	L_∞ -norm	L_2 -norm	L_∞ -norm
0.1	8.56447e-06	1.06174e-03	8.33926e-06	1.14140e-03
0.2	1.13259e-05	1.80386e-03	1.11443e-05	1.87280e-03
0.3	1.34809e-05	2.46325e-03	1.33529e-05	2.52667e-03
0.4	1.54954e-05	3.07668e-03	1.54042e-05	3.13596e-03
0.5	1.74075e-05	3.64429e-03	1.73374e-05	3.69857e-03
0.6	1.91941e-05	4.16207e-03	1.91346e-05	4.21119e-03
0.7	2.08362e-05	4.62956e-03	2.07809e-05	4.67387e-03
0.8	2.23256e-05	5.04855e-03	2.22705e-05	5.08817e-03
0.9	2.36619e-05	5.42156e-03	2.36049e-05	5.45689e-03
1.0	2.46120e-05	5.78314e-03	2.47896e-05	5.78346e-03

Table 14 Comparison of L_2 -norm L_∞ -norm and GRE with respect to space and time partitions for Example 6.5 at $T = 0.5$

Time		$N = 20$	$N = 40$	$N = 60$	$N = 80$
$\Delta t = 0.1$	L_2 -norm	2.69111e-04	3.41167e-05	1.20233e-05	6.11513e-06
	L_∞ -norm	5.88431e-03	3.91978e-03	3.59510e-03	3.48590e-03
	GRE	5.37349e-02	3.58310e-02	3.25095e-02	3.13709e-02
$\Delta t = 0.01$	L_2 -norm	2.38562e-04	3.04466e-05	1.09433e-05	5.63647e-06
	L_∞ -norm	5.93525e-03	3.91185e-03	3.58612e-03	3.47732e-03
	GRE	5.36526e-02	3.57576e-02	3.24471e-02	3.13131e-02
$\Delta t = 0.001$	L_2 -norm	2.39638e-04	3.08817e-05	1.11036e-05	5.71202e-06
	L_∞ -norm	5.93765e-03	3.91218e-03	3.58625e-03	3.47738e-03
	GRE	5.36635e-02	3.57629e-02	3.24500e-02	3.13151e-02

and L_∞ norm can be observed along the column of Table 13. Again, the effect of perturbation parameters on L_2 -norm, L_∞ -norm and GRE has been studied in Table 14. It is observed that the increment in the non-linearity of polynomial $f(u)$ does not effect the approximation efficiency and accuracy. Parameter uniform rate of convergence of order two has been reported in Table 15 with $\Delta t = 10^{-2}$.

Example 6.6 Consider the fourth order differential equation having bistable cubic non-linearity

$$u_t + \epsilon u_{\zeta\zeta\zeta\zeta} - u_{\zeta\zeta} = u(u - \alpha)(1 - u) \quad (\zeta, t) \in [a, b] \times [0, T], \tag{57}$$

Table 15 Parameter uniform convergence rate at $T = 0.2$ for Example 6.5

ϵ	$N = 5$	$N = 10$	$N = 20$	$N = 40$	$N = 80$
10^0	0.027097829	0.006278871	0.001656379	0.000414531	0.000103733
10^{-1}	0.04799501	0.016872231	0.004031238	0.001016282	0.000255155
10^{-2}	0.045440459	0.024649882	0.007400184	0.001811592	0.000454294
10^{-3}	0.045353053	0.025807968	0.008589973	0.002413281	0.000598185
10^{-4}	0.045512133	0.025971564	0.008671138	0.002484271	0.000689575
10^{-5}	0.045528756	0.025983209	0.008669169	0.002492881	0.000685876
E_n	0.04799501	0.025983209	0.008671138	0.002492881	0.000689575
R_n	0.885304799	1.583286368	1.798407329	1.854034639	–

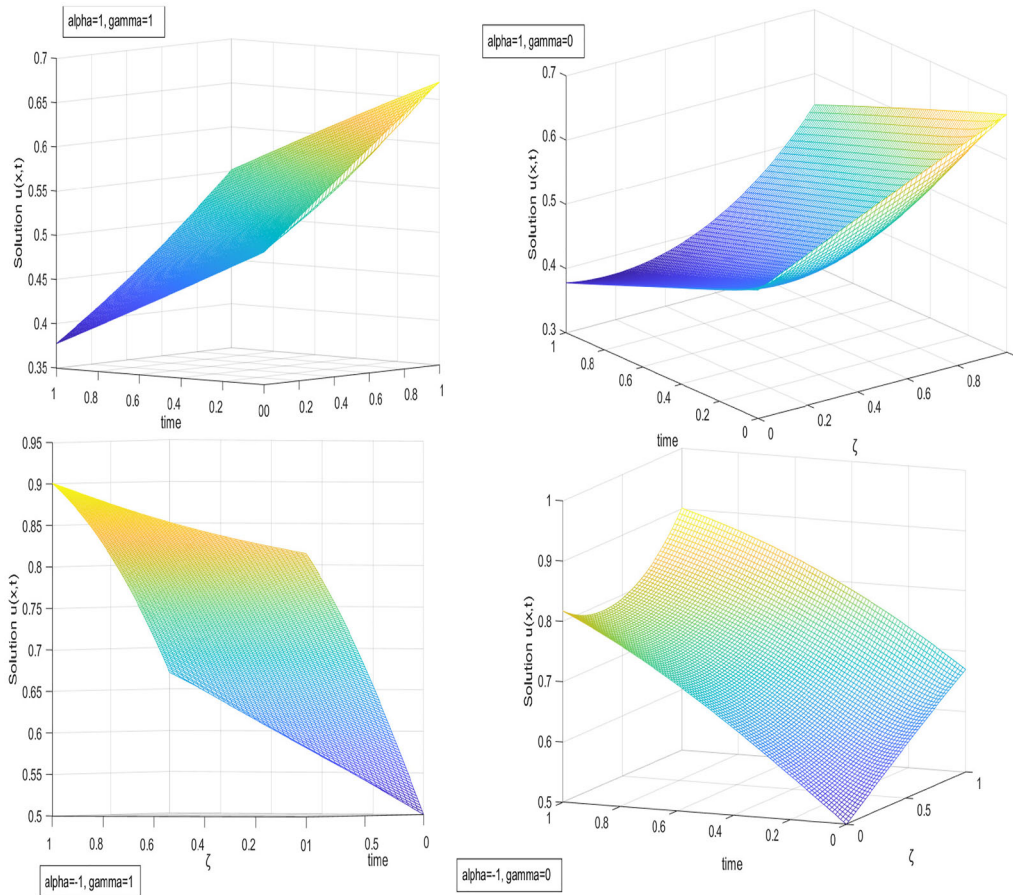


Fig. 12 Solution profile of Example 6.6 for different values of γ and α

with the initial and boundary conditions

$$u(\zeta, 0) = \frac{1}{2} + \frac{1}{2} \tanh\left(\frac{\sqrt{2}\zeta}{4}\right),$$

$$u(a, t) = \frac{1}{2} + \frac{1}{2} \tanh\left(\frac{\sqrt{2}a + (1 - 2\alpha)t}{4}\right),$$

$$u(b, t) = \frac{1}{2} + \frac{1}{2} \tanh\left(\frac{\sqrt{2}b + (1 - 2\alpha)t}{4}\right).$$

Table 16 L_2 -norm and L_∞ -norm with $\Delta t = 0.01$ and $N = 32$, $\alpha = 1$ for Example 6.6

Time	$\varepsilon = 1$		$\varepsilon = 0.1$		$\varepsilon = 0.001$	
	L_2 -norm	L_∞ -norm	L_2 -norm	L_∞ -norm	L_2 -norm	L_∞ -norm
0.0	1.75315e-02	6.64514e-01	1.75315e-02	6.64514e-01	1.75315e-02	6.64514e-01
0.1	1.72000e-02	6.51753e-01	1.70980e-02	6.47390e-01	1.69815e-02	6.42528e-01
0.2	1.69010e-02	6.40410e-01	1.67894e-02	6.35634e-01	1.66406e-02	6.29654e-01
0.3	1.65980e-02	6.28916e-01	1.64890e-02	6.24250e-01	1.63325e-02	6.18006e-01
0.4	1.62911e-02	6.17275e-01	1.61859e-02	6.12772e-01	1.60308e-02	6.06588e-01
0.5	1.59806e-02	6.05495e-01	1.58793e-02	6.01159e-01	1.57281e-02	5.95136e-01
0.6	1.56667e-02	5.93590e-01	1.55692e-02	5.89418e-01	1.54229e-02	5.83585e-01
0.7	1.53498e-02	5.81571e-01	1.52561e-02	5.77561e-01	1.51147e-02	5.71925e-01
0.8	1.50302e-02	5.69451e-01	1.49402e-02	5.65600e-01	1.48039e-02	5.60161e-01
0.9	1.47083e-02	5.57246e-01	1.46220e-02	5.53549e-01	1.44906e-02	5.48306e-01
1.0	1.43845e-02	5.44968e-01	1.43017e-02	5.41423e-01	1.41752e-02	5.36373e-01

Table 17 Computed L_2 -norm and L_∞ -norm with $\Delta t = 0.01$ and $N = 50$ and $\alpha = -1$ for Example 6.6

Time	$\varepsilon = 1$		$\varepsilon = 0.1$		$\varepsilon = 0.0001$	
	L_2 -norm	L_∞ -norm	L_2 -norm	L_∞ -norm	L_2 -norm	L_∞ -norm
0.0	1.12484e-02	6.66408e-01	1.12484e-02	6.66408e-01	1.12484e-02	6.66408e-01
0.1	1.17873e-02	6.98307e-01	1.17722e-02	6.97298e-01	1.17533e-02	6.96037e-01
0.2	1.23016e-02	7.28806e-01	1.22826e-02	7.27537e-01	1.22555e-02	7.25730e-01
0.3	1.27819e-02	7.57292e-01	1.27609e-02	7.55890e-01	1.27291e-02	7.53767e-01
0.4	1.32265e-02	7.83668e-01	1.32038e-02	7.82148e-01	1.31688e-02	7.79813e-01
0.5	1.36350e-02	8.07897e-01	1.36105e-02	8.06262e-01	1.35729e-02	8.03753e-01
0.6	1.40074e-02	8.29995e-01	1.39812e-02	8.28245e-01	1.39412e-02	8.25580e-01
0.7	1.43448e-02	8.50014e-01	1.43169e-02	8.48152e-01	1.42747e-02	8.45341e-01
0.8	1.46485e-02	8.68042e-01	1.46191e-02	8.66073e-01	1.45749e-02	8.63125e-01
0.9	1.49206e-02	8.84189e-01	1.48896e-02	8.82118e-01	1.48435e-02	8.79042e-01
1.0	1.51630e-02	8.98581e-01	1.51306e-02	8.96414e-01	1.50827e-02	8.93220e-01

For $\varepsilon = 1$ and $\alpha = 1$ and -1 , the travelling wave configuration has been observed. For $\varepsilon = 1$ the travelling wave have a constant phase but as γ decreases i.e. for $\varepsilon = 0$ the wave configuration has some phase turning point as can be observed from the Fig. 12 which shows the boundary layer effect due to perturbation parameter ε . It has also been observed that for positive α the solution profile has decreasing nature while for negative α the wave profile is increasing with time, can be observed along the column in Tables 16 and 17. The effect of perturbation parameter can be observed from any row of the Tables 16 and 17 for both the cases $\alpha = 1$ and $\alpha = -1$.

7 Conclusions and discussion

The proposed technique has been implemented to various forms of fourth order semi-linear dissipative, reaction–diffusion equations which are analysed with fairly known initial functions. Travelling wave behaviour propagating in reaction–diffusion dissipative media has been studied using the proposed hybrid technique. For problems having exact form of solution the error in the form of L_2 norm and L_∞ norm has been reported in tables. These equations have mono-stable and bi-stable non-linearity.

Error analysis shows that the hybrid technique is significantly effective for higher order problems with higher degree of non-linearity.

The equations exhibited wave behaviour and the effect of perturbation parameter has been studied. In Example 3 non-linear fourth order problem with Fisher equation type non-linearity has been considered. Effect of the bounded domain on the wave behaviour has also been observed. In Example 6 fourth order equation with bi-stable cubic non-linearity has been considered. The effect of perturbation parameter ε and the parameter α has been studied. Both the equations model the problems in population dynamics. These mono-stable and bi-stable non-linear problems have travelling wave configurations. Parameter Uniform convergence rate has been studied for analysing the effect of perturbation parameter ε and the rate of convergence in certain cases found to be greater than 1.



Acknowledgements The Authors are thankful to the reviewers for their valuable comments.

Open Access This article is licensed under a Creative Commons Attribution 4.0 International License, which permits use, sharing, adaptation, distribution and reproduction in any medium or format, as long as you give appropriate credit to the original author(s) and the source, provide a link to the Creative Commons licence, and indicate if changes were made. The images or other third party material in this article are included in the article's Creative Commons licence, unless indicated otherwise in a credit line to the material. If material is not included in the article's Creative Commons licence and your intended use is not permitted by statutory regulation or exceeds the permitted use, you will need to obtain permission directly from the copyright holder. To view a copy of this licence, visit <http://creativecommons.org/licenses/by/4.0/>.

Funding The authors declare that no funds, grants, or other support were received during the preparation of this manuscript.

Data availability statement Not applicable.

Declarations

Author contributions Priyanka Priyanka and Shelly Arora contributed to conceptualization and methodology of the manuscript. Saroj Sahani and Fateh Mebarek-Oudina contributed to the preparation and editing of the manuscript.

Conflict of interest The authors have no relevant financial or non-financial interests to disclose.

Informed consent Not applicable.

References

1. Abbasbandy, S.: Numerical solution of non-linear Klein–Gordon equations by variational iteration method. *Int. J. Numer. Methods Eng.* **70**(7), 876–881 (2007)
2. Abbasbandy, S.; Asady, B.: Newton's method for solving fuzzy nonlinear equations. *Appl. Math. Comput.* **159**(2), 349–356 (2004)
3. Abbaszadeh, M.; Dehghan, M.; Khodadadian, A.; Heitzinger, C.: Error analysis of interpolating element free Galerkin method to solve non-linear extended Fisher–Kolmogorov equation. *Comput. Math. Appl.* **80**(1), 247–262 (2020)
4. Abo-Dahab, S.M.; Abdelhafez, M.A.; Mebarek-Oudina, F.; Bilal, S.M.: MHD Casson nanofluid flow over nonlinearly heated porous medium in presence of extending surface effect with suction/injection. *Indian J. Phys.* **95**(12), 2703–2717 (2021)
5. Alba-Fernández, V.; Ibáñez-Pérez, M.J.; Jiménez-Gamero, M.D.: A bootstrap algorithm for the two-sample problem using trigonometric Hermite spline interpolation. *Commun. Nonlinear Sci. Numer. Simul.* **9**(2), 275–286 (2004)
6. Aronson, D.G.; Weinberger, H.F.: Multidimensional nonlinear diffusion arising in population genetics. *Adv. Math.* **30**(1), 33–76 (1978)
7. Arora, G.; Joshi, V.: Simulation of generalized nonlinear fourth order partial differential equation with quintic trigonometric differential quadrature method. *Math. Models Comput. Simul.* **11**(6), 1059–1083 (2019)
8. Arora, S.; Kaur, I.: An efficient scheme for numerical solution of Burgers' Equation using quintic Hermite interpolating polynomials. *Arab. J. Math.* **5**(1), 23–34 (2016)
9. Arora, U.; Karaa, S.; Mohanty, R.K.: A new stable variable mesh method for 1-D non-linear parabolic partial differential equations. *Appl. Math. Comput.* **181**(2), 1423–1430 (2006)
10. Arora, S.; Dhaliwal, S.S.; Kukreja, V.K.: Computationally efficient technique for weight functions and effect of orthogonal polynomials on the average. *Appl. Math. Comput.* **186**(1), 623–631 (2007)
11. Arora, S.; Kaur, I.; Tilahun, W.: An exploration of quintic Hermite splines to solve Burgers' equation. *Arab. J. Math.* **9**(1), 19–36 (2020)
12. Arora, S.; Jain, R.; Kukreja, V.K.: Solution of Benjamin–Bona–Mahony–Burgers equation using collocation method with quintic Hermite splines. *Appl. Numer. Math.* **154**, 1–16 (2020)
13. Başhan, A.; Ucar, Y.; Yağmurlu, N.M.; Esen, A.: Numerical solutions for the fourth order extended Fisher–Kolmogorov equation with high accuracy by differential quadrature method. *Sigma J. Eng. Nat. Sci.* **9**(3), 273–284 (2018)
14. Belmonte-Beitia, J.; Calvo, G.F.; Perez-Garcia, V.M.: Effective particle methods for Fisher–Kolmogorov equations: theory and applications to brain tumor dynamics. *Commun. Nonlinear Sci. Numer. Simul.* **19**(9), 3267–3283 (2014)
15. Bhal, S.K.; Danumjaya, P.; Fairweather, G.: The Crank–Nicolson orthogonal spline collocation method for one-dimensional parabolic problems with interfaces. *J. Comput. Appl. Math.* **383**, 113–119 (2021)
16. Clark, V.; Meyer, J.C.: On two-signed solutions to a second order semi-linear parabolic partial differential equation with non-Lipschitz nonlinearity. *J. Differ. Equ.* **269**(2), 1401–1431 (2020)
17. Clavero, C.; Jorge, J.C.; Lisbona, F.: A uniformly convergent scheme on a nonuniform mesh for convection–diffusion parabolic problems. *J. Comput. Appl. Math.* **154**(2), 415–429 (2003)
18. Couillet, P.; Huerre, P.: *New Trends in Nonlinear Dynamics and Pattern-Forming Phenomena: The Geometry of Nonequilibrium*, vol. 237. Springer Science & Business Media, Berlin (2012)
19. Couillet, P.; Elphick, C.; Repaux, D.: Nature of spatial chaos. *Phys. Rev. Lett.* **58**(5), 431 (1987)
20. Danumjaya, P.; Pani, A.K.: Finite element methods for the extended Fisher–Kolmogorov equation. Research Report: IMG-RR-2002-3, Industrial Mathematics Group, Department of Mathematics, IIT, Bombay(2002)
21. Danumjaya, P.; Pani, A.K.: Orthogonal cubic spline collocation method for the extended Fisher–Kolmogorov equation. *J. Comput. Appl. Math.* **174**(1), 101–117 (2005)
22. Danumjaya, P.; Pani, A.K.: Numerical methods for the extended Fisher–Kolmogorov (EFK) equation. *Int. J. Numer. Anal. Model.* **3**(2), 186–210 (2006)



23. Dee, G.T.; Van Saarloos, W.: Bistable systems with propagating fronts leading to pattern formation. *Phys. Rev. Lett.* **60**(25), 2641 (1988)
24. Dehghan, M.; Hooshyarfarzin, B.; Abbaszadeh, M.: Numerical simulation based on a combination of finite-element method and proper orthogonal decomposition to prevent the groundwater contamination. *Eng. Comput.* **38**(4), 3445–3461 (2022)
25. Dehghan, M.; Shafieeabyaneh, N.: Local radial basis function-finite-difference method to simulate some models in the nonlinear wave phenomena: regularized long-wave and extended Fisher–Kolmogorov equations. *Eng. Comput.* **37**(2), 1159–1179 (2021)
26. Elliott, C.M.; French, D.A.; Milner, F.A.: A second order splitting method for the Cahn–Hilliard equation. *Numerische Mathematik* **54**(5), 575–590 (1989)
27. Field, R.J.: *Oscillations and Traveling Waves in Chemical Systems*. Wiley, New York (1985)
28. Fisher, R.A.: The wave of advance of advantageous genes. *Ann. Eugen.* **7**(4), 355–369 (1937)
29. Focant, S.; Gallay, Th.: Existence and stability of propagating fronts for an autocatalytic reaction–diffusion system. *Phys. D: Nonlinear Phenom.* **120**(3–4), 346–368 (1998)
30. Gavete, L.; Ureña, F.; Benito, J.J.; García, A.; Ureña, M.; Salet, E.: Solving second order non-linear elliptic partial differential equations using generalized finite difference method. *J. Comput. Appl. Math.* **318**, 378–387 (2017)
31. Gudi, T.; Gupta, H.S.: A fully discrete C0 interior penalty Galerkin approximation of the extended Fisher–Kolmogorov equation. *J. Comput. Appl. Math.* **247**, 1–16 (2013)
32. Hall, C.A.: On error bounds for spline interpolation. *J. Approx. Theory* **1**(2), 209–218 (1968)
33. Hornreich, R.M.; Luban, M.; Shtrikman, S.: Critical behavior at the onset of \mathbf{k} -space instability on the λ line. *Phys. Rev. Lett.* **35**(25), 1678 (1975)
34. Jaiswal, S.; Chopra, M.; Das, S.: Numerical solution of non-linear partial differential equation for porous media using operational matrices. *Math. Comput. Simul.* **160**, 138–154 (2019)
35. Kaliappan, P.: An exact solution for travelling waves of $u_t = Du_{xx} + u - u^k$. *Phys. D: Nonlinear Phenom.* **11**(3), 368–374 (1984)
36. Kalies, W.D.; Kwapisz, J.; VanderVorst, R.C.A.M.: Homotopy classes for stable connections between Hamiltonian saddle-focus equilibria. *Commun. Math. Phys.* **193**(2), 337–371 (1998)
37. Kaur, D.; Mohanty, R.K.: Two-level implicit high order method based on half-step discretization for 1D unsteady biharmonic problems of first kind. *Appl. Numer. Math.* **139**, 1–14 (2019)
38. Knibb, D.; Scraton, R.E.: A collocation method for the numerical solution of non-linear parabolic partial differential equations. *IMA J. Appl. Math.* **22**(3), 305–315 (1978)
39. Kudryashov, N.A.: Quasi-exact solutions of the dissipative Kuramoto–Sivashinsky equation. *Appl. Math. Comput.* **219**(17), 9213–9218 (2013)
40. Kumar, D.; Kadalbajoo, M.K.: A parameter-uniform numerical method for time-dependent singularly perturbed differential-difference equations. *Appl. Math. Model.* **35**(6), 2805–2819 (2011)
41. Majeed, A.; Kamran, M.; Abbas, M.; Singh, J.: An efficient numerical technique for solving time-fractional generalized Fisher’s equation. *Front. Phys.* **8**, 293 (2020)
42. Mansour, M.B.A.: Traveling wave patterns in nonlinear reaction–diffusion equations. *J. Math. Chem.* **48**(3), 558–565 (2010)
43. Mazure, M.L.: On the Hermite interpolation. *Comptes Rendus Mathématique* **340**(2), 177–180 (2005)
44. Mebarek-Oudina, F.: Convective heat transfer of Titania nanofluids of different base fluids in cylindrical annulus with discrete heat source. *Heat Transf. Asian Res.* **48**(1), 135–147 (2019)
45. Miller, J.J.H.; O’riordan, E.; Shishkin, G.I.: *Fitted Numerical Methods for Singular Perturbation Problems: Error Estimates in the Maximum Norm for Linear Problems in One and Two Dimensions*. World Scientific, Singapore (1996)
46. Mittal, R.C.; Dahiya, S.: A study of quintic B-spline based differential quadrature method for a class of semi-linear Fisher–Kolmogorov equations. *Alex. Eng. J.* **55**(3), 2893–2899 (2016)
47. Peletier, L.A.; Troy, W.C.: Spatial patterns described by the extended Fisher–Kolmogorov (EFK) equation: kinks. *Differ. Integral Equ.* **8**(6), 1279–1304 (1995)
48. Peletier, L.A.; Troy, W.C.: A topological shooting method and the existence of kinks of the extended Fisher–Kolmogorov equation. *Topol. Methods Nonlinear Anal.* **6**(2), 331–355 (1995)
49. Peletier, L.A.; Troy, W.C.: Chaotic spatial patterns described by the extended Fisher–Kolmogorov equation. *J. Differ. Equ.* **129**(2), 458–508 (1996)
50. Peletier, L.A.; Troy, W.C.: Spatial patterns described by the extended Fisher–Kolmogorov equation: periodic solutions. *SIAM J. Math. Anal.* **28**(6), 1317–1353 (1997)
51. Peletier, L.A.; Troy, W.C.; Van der Vorst, R.C.A.M.: Stationary solutions of a fourth order nonlinear diffusion equation. *Differ. Equ.* **31**(2), 301–314 (1995)
52. Prenter, P.M.: *Splines and Variational Methods*. Wiley, New York (1975)
53. Rajan, M.P.; Reddy, G.D.: A generalized regularization scheme for solving singularly perturbed parabolic PDEs. *Partial Differ. Equ. Appl. Math.* **5**, 100270 (2022)
54. Rohila, R.; Mittal, R.C.: A numerical study of two-dimensional coupled systems and higher order partial differential equations. *Asian Eur. J. Math.* **12**(05), 1950071 (2019)
55. Rottschäfer, V.: Multi-bump patterns by a normal form approach. *Discret. Contin. Dyn. Syst. B* **1**(3), 363 (2001)
56. Rottschäfer, V.; Doelman, A.: On the transition from the Ginzburg–Landau equation to the extended Fisher–Kolmogorov equation. *Phys. D: Nonlinear Phenom.* **118**(3–4), 261–292 (1998)
57. Rottschäfer, V.; Wayne, C.E.: Existence and stability of traveling fronts in the extended Fisher–Kolmogorov equation. *J. Differ. Equ.* **176**(2), 532–560 (2001)
58. Rubin, S.G.; Graves, R.A.: *A Cubic Spline Approximation for Problems in Fluid Mechanics*. National Aeronautics and Space Administration, Washington, D.C. (1975)
59. Samir, I.; Badra, N.; Seadawy, A.R.; Ahmed, H.M.; Arnous, A.H.: Exact wave solutions of the fourth order non-linear partial differential equation of optical fiber pulses by using different methods. *Optik* **230**, 166313 (2021)



60. Sousa, E.; Li, C.: A weighted finite difference method for the fractional diffusion equation based on the Riemann–Liouville derivative. *Appl. Numer. Math.* **90**, 22–37 (2015)
61. Stokes, A.N.: Nonlinear diffusion waveshapes generated by possibly finite initial disturbances. *J. Math. Anal. Appl.* **61**(2), 370–381 (1977)
62. Valentin, C.; Couenne, F.; Jallut, C.; Choubert, J.M.; Tayakout-Fayolle, M.: Dynamic modeling of a batch sludge settling column by partial differential non linear equations with a moving interface. *IFAC-PapersOnLine* **54**(3), 13–18 (2021)
63. van den Berg, J.B.: Uniqueness of solutions for the extended Fisher–Kolmogorov equation. *Comptes Rendus de l’Académie des Sciences-Series I-Mathematics* **326**(4), 447–452 (1998)
64. Van Saarloos, W.: Dynamical velocity selection: marginal stability. *Phys. Rev. Lett.* **58**(24), 2571 (1987)
65. Wang, J.; Li, H.; He, S.; Gao, W.; Liu, Y.: A new linearized Crank–Nicolson mixed element scheme for the extended Fisher–Kolmogorov equation. *Sci. World J.* **2013**, 1–11 (2013). <https://doi.org/10.1155/2013/756281>
66. Zhou, Q.; Ekici, M.; Sonmezoglu, A.; Manafian, J.; Khaleghizadeh, S.; Mirzazadeh, M.: Exact solitary wave solutions to the generalized Fisher equation. *Optik* **127**(24), 12085–12092 (2016)
67. Zimmermann, W.: Propagating fronts near a Lifshitz point. *Phys. Rev. Lett.* **66**(11), 1546 (1991)

Publisher’s Note Springer Nature remains neutral with regard to jurisdictional claims in published maps and institutional affiliations.

